

Infrared point source variability between the Spitzer and MSX surveys of the Galactic mid-plane

Thomas P. Robitaille¹, Martin Cohen², Barbara A. Whitney³, Marilyn Meade⁴, Brian Babler⁴, Remy Indebetouw⁵, Ed Churchwell⁴

ABSTRACT

We present a list of 552 sources with suspected variability, based on a comparison of mid-infrared photometry from the GLIMPSE I and MSX surveys, which were carried out nearly a decade apart. We were careful to address issues such as the difference in resolution and sensitivity between the two surveys, as well as the differences in the spectral responses of the instruments. We selected only sources where the IRAC $8.0\mu\text{m}$ and MSX $8.28\mu\text{m}$ fluxes differ by more than a factor of two, in order to minimize contamination from sources where the difference in fluxes at $8\mu\text{m}$ is due to a strong $10\mu\text{m}$ silicate feature. We present a subset of 40 sources for which additional evidence suggests variability, using 2MASS and MIPS GAL data. Based on a comparison with the variability flags in the IRAS and MSX Point-Source Catalogs we estimate that at least a quarter of the 552 sources, and at least half of the 40 sources are truly variable. In addition, we tentatively confirm the variability of one source using multi-epoch IRAS LRS spectra. We suggest that most of the sources in our list are likely to be Asymptotic Giant Branch stars.

Subject headings: infrared: stars — stars: AGB and post-AGB — stars: pre-main-sequence — stars: variables: other — surveys

¹SUPA, School of Physics and Astronomy, University of St Andrews, North Haugh, KY16 9SS, St Andrews, United Kingdom; tr9@st-andrews.ac.uk

²Radio Astronomy Laboratory, 601 Campbell Hall, University of California at Berkeley, Berkeley, CA 94720; mcohen@astro.berkeley.edu

³Space Science Institute, 4750 Walnut St. Suite 205, Boulder, CO 80301, USA; bwhitney@spacescience.org

⁴Department of Astronomy, 475 North Charter St., University of Wisconsin, Madison, WI 53706; meade@astro.wisc.edu, brian@sal.wisc.edu, ebc@astro.wisc.edu

⁵Spitzer Fellow, University of Virginia, Astronomy Dept., P.O. Box 3818, Charlottesville, VA, 22903-0818; remy@virginia.edu

1. Introduction

The Combined General Catalog of Variable Stars (GCVS4.2 ; Samus & Durlevich 2004) lists 38,624 confirmed variable sources, most of which are located in the Milky-Way Galaxy. The types of variable sources are numerous, ranging from eruptive (e.g. FU Orionis objects) or pulsating (e.g. Cepheid, Mira, or RR Lyrae) variables to eclipsing binaries or cataclysmic variables. Most of these have been found through optical surveys, which are limited in depth by dust extinction in our own Galaxy. Thus, looking in the direction of the Galactic plane, these sources are likely to be within a kpc from the sun.

Searching for variability at mid-IR wavelengths has two advantages. First, the much reduced extinction at mid-IR wavelengths means that bright stars can be seen to much larger distances. Second, dust emission is much brighter at mid-IR wavelengths than at shorter wavelengths, and therefore we can search for variability in dusty objects such as Asymptotic Giant Branch (AGB) stars or Young Stellar Objects (YSOs).

Data from the IRAS satellite were used to assign variability likelihoods to sources in the IRAS Point Source Catalog (the **Var** index). This was made possible by the fact that most areas of the sky were observed at least twice, with observations typically separated by weeks to months. Thousands of new variable stars were discovered, most of which lie in the Galactic plane or in the Galactic bulge (Spear et al. 1993). However, the low sensitivity and resolution of the IRAS observations along with source confusion meant that only the brightest sources were found in the Galactic mid-plane (most sources in the IRAS Point-Source Catalog with $|b| < 1^\circ$ and a **Var** index larger than 98% - indicating very likely variability - have $F_{12\mu\text{m}} > 1\text{Jy}$).

The *Midcourse Space Experiment* (MSX) satellite, launched in 1996, completed a survey of the Galactic plane (Price et al. 2001) from 8 to $21\mu\text{m}$, with improved sensitivity and spatial resolution over IRAS. Most areas of the Galactic plane were observed multiple times (typically four times) within a few months. Each source in the MSX Point Source Catalog was then assigned a variability flag in each band (i.e. **vara**, **varc**, **vard**, and **vare**).

More recently, the Galactic plane was surveyed in the mid-IR by the *Spitzer Space Telescope* (Werner et al. 2004), launched in 2003. *Spitzer* carried out the Galactic Legacy Infrared Mid-Plane Survey Extraordinaire (GLIMPSE I; Benjamin et al. 2003) and the MIPS Inner Galactic Plane Survey (MIPSGAL; PI: Carey) using the InfraRed Array Camera (IRAC; 3.6 to $8.0\mu\text{m}$; Fazio et al. 2004) and the Multiband Imaging Photometer for Spitzer (MIPS; 24 to $160\mu\text{m}$; Rieke et al. 2004) respectively.

Both the MSX and GLIMPSE I surveys include observations around $8\mu\text{m}$, and were taken ~ 8 years apart. In this paper we make use of this similarity in wavelengths to search

for sources with mid-IR variability between the MSX and the *Spitzer* surveys. Our analysis is most sensitive to variability arising from dusty objects such as AGB stars or YSOs, and should be sensitive to sources with a wide range of variability timescales extending up to a decade.

In §2, we give a summary of the various datasets used for this study. In §3, we give an overview of the procedure used to select the sample of candidate variable stars. In particular, we discuss the possible sources of contamination, i.e. sources that look - but are not - variable (§3.1); the issue of apparent variability due to strong spectral features and the differences in spectral responses (§3.2); and the details of the merging of the MSX and GLIMPSE I catalogs (§3.3). In §3.4 we compile a final list of candidate variable stars. We then attempt to refine this sample to a subset of sources that present additional evidence for potential variability (§4.1), and present Spectral Energy Distributions (SEDs) of the 40 sources in this subset, as well as images for three typical sources (§4.2). Finally we discuss the possible nature of these sources (§5) and summarize our results (§6).

2. Observations

In order to search for point source variability, we made use of the following data:

- The MSX survey of the Galactic plane (Price et al. 2001), which was carried out between 1996 and 1997, and consisted of imaging in four bands: A ($8.28\mu\text{m}$), C ($12.13\mu\text{m}$), D ($14.65\mu\text{m}$), and E ($21.3\mu\text{m}$).
- The 2 Micron All-Sky Survey (2MASS; Skrutskie et al. 2006), which was carried out between 1997 and 2001. The observations consist of imaging in three bands: J ($1.25\mu\text{m}$), H ($1.65\mu\text{m}$), and K_s ($2.15\mu\text{m}$).
- The GLIMPSE I survey of the Galactic mid-plane (Benjamin et al. 2003), which was carried out in 2004 at 3.6, 4.5, 5.8, and $8.0\mu\text{m}$ using the IRAC instrument on board *Spitzer*.
- The MIPS GAL survey of the same region as GLIMPSE I, carried out in 2005 and 2006 at 24, 70, and $160\mu\text{m}$ using the MIPS instrument on board *Spitzer*. We make use only of the data taken at $24\mu\text{m}$.

The resolution of 2MASS and IRAC is $\sim 2''$, that of MIPS is $\sim 10''$, and the resolution of the MSX observations is $\sim 18''$.

The approximate sensitivity and saturation levels for the various datasets are listed in Table 1. The values most critical for this work are the saturation level of IRAC $8.0\mu\text{m}$ (1590mJy) and the sensitivity level of MSX $8.28\mu\text{m}$ (100 to 200mJy).

The absolute calibrations of the observations are described in detail in Cohen et al. (2003), Reach et al. (2005), Engelbracht et al. (2007), and Price et al. (2004) for 2MASS, IRAC, MIPS $24.0\mu\text{m}$, and MSX respectively.

The spectral response curves of the instruments used for the various datasets are shown in Figure 1. In this paper we make use of the similarity between the wavelength range covered by IRAC $8.0\mu\text{m}$ and MSX $8.28\mu\text{m}$ (as well as the similarity between MIPS $24.0\mu\text{m}$ and MSX $21.3\mu\text{m}$ in §4.1).

We used the GLIMPSE v2.0 Point-Source Catalog (Meade et al., 2007¹), which includes IRAC fluxes for all the point sources in the survey, as well as 2MASS fluxes when available. We chose the Point Source Catalog over the Point Source Archive as it has a higher reliability and does not include saturated sources (for a more detailed description of the Catalogs and Archives, we refer the reader to Meade et al., 2007). For MSX data, we used the MSX6C Point Source Catalog (Egan et al. 2003). We restricted our analysis to the (ℓ, b) ranges covered by GLIMPSE I, i.e. $10^\circ < |\ell| < 65^\circ$ and $|b| < 1^\circ$. The total area covered is 220 square degrees.

3. The selection of the variable star candidates

3.1. Contaminants

In order to search for variable stars in the mid-infrared, we would ideally use observations of the Galactic plane at two different epochs taken with the same telescope and with the same filters. However, in this case we have data for two surveys using *similar* but not *identical* spectral responses, namely IRAC $8.0\mu\text{m}$ and MSX $8.28\mu\text{m}$, at spatial resolutions differing by almost a factor of 10, and sensitivity and saturation limits overlapping by only an order of magnitude. Therefore, great care has to be taken when comparing the two datasets.

There are three main sources of possible contamination, i.e. sources that could look variable between IRAC $8.0\mu\text{m}$ and MSX $8.28\mu\text{m}$ based on a comparison of the images or catalogs:

¹http://www.astro.wisc.edu/glimpse/glimpse1_dataproduct_v2.0.pdf

Confusion The difference in the resolutions between MSX and IRAC observations (18" and 2" respectively) means that multiple sources in IRAC 8.0 μ m can appear as one source in MSX 8.28 μ m. Therefore, if one were to merge an MSX source with the closest IRAC source, one might find that the fluxes appear to differ, when in fact this is because other nearby sources in IRAC also contribute to the flux of the MSX source.

Saturation If a source is mildly saturated in IRAC 8.0 μ m, the response of the detector becomes nonlinear, and the source will appear fainter than it really is. Since MSX has a much lower sensitivity, many sources detected in MSX are saturated in GLIMPSE, so this effect could be common. Therefore, we choose to use the GLIMPSE Catalog, which does not include saturated sources. More generally, since we can use only very bright (non saturated) sources in GLIMPSE and faint sources in MSX, it is essential in this analysis to perform a rigorous quality check of all fluxes by inspecting the images to ensure there are no ‘false sources’ or other technical problems linked to saturation or noise that could affect flux measurements.

Spectral features Since IRAC 8.0 μ m and MSX 8.28 μ m do not cover exactly the same wavelength range (as shown in Figure 1), the two fluxes for a same source may differ if the spectrum contains strong spectral features in the wavelength range covered by the instruments. For example, YSOs with a strong silicate feature at 10 μ m in absorption (e.g. embedded protostars), or in emission (e.g. young stars with disks), are likely to be affected by this. This effect will also be present in stars with large amounts of interstellar extinction, which produces a silicate absorption feature at 10 μ m. In addition, the presence of strong emission or absorption features in the wavelength ranges covered by only one or the other of the instruments would also lead to differences in the fluxes. For example, the 6-6.5 μ m region is covered only by MSX 8.28 μ m, and cool giants and supergiants are known to show absorption at 6.3 μ m due to the H₂O absorption bands (Cohen et al. 1995; Tsuji 2001, 2003).

These issues mean that it would be extremely difficult to produce a statistically *complete* sample of variable star candidates. Instead for this work we choose to prioritize *reliability* over completeness.

3.2. Strong spectral features and apparent variability

As mentioned in §3.1, strong spectral features in the wavelength range covered by the IRAC 8.0 μ m and MSX 8.28 μ m bandpasses could cause the two fluxes to differ. In order to assess how important this effect is for YSOs, we use the publicly available grid of 200,000 YSO model SEDs from Robitaille et al. (2006). We use the convolved IRAC and MSX fluxes for each model for a \sim 18,000 AU aperture, which corresponds to 18'' (the resolution of the MSX observations) at 1kpc (a typical distance to objects in the GLIMPSE survey). We note that the choice of aperture has very little effect for the analysis presented here.

The left panel in Figure 3 shows a histogram of the number of models as a function of the ratio of the IRAC 8.0 μ m flux to the MSX 8.28 μ m flux for all the models. Only for very few models (0.15%) do the two fluxes differ by more than a factor of two. We note that although we use only YSO models for this analysis, results for AGB models are likely to be similar, since both types of objects show similar SEDs, i.e. thermal dust emission with a silicate feature.

We then investigated how much the ratio of IRAC 8.0 μ m to MSX 8.28 μ m for a normal star would be affected by interstellar extinction. To do this we used a 4,000 K model atmosphere from Castelli & Kurucz (2004) with $\text{Log}[g]=+2.0$ and $\text{Log}[Z/H]=-2.0$, to which we applied extinctions of $A_V=0, 20, 40, 60, 80,$ and 100 using the extinction law discussed in Robitaille et al. (2007). We do not expect the interstellar extinction towards most sources to exceed this value, since A_V values of 100 or more are only seen through InfraRed Dark Clouds (IRDCs). Such sources would be easy to identify, since IRDCs are clearly visible against the background diffuse PAH emission: indeed, assuming $A_{[8.0]}/A_{K_s} \approx 0.5$ (Flaherty et al. 2007) and $A_{K_s}/A_V \approx 0.1$ (Cardelli et al. 1989), $A_V=100$ corresponds to $A_{[8.0]} \approx 5$, i.e. a drop in brightness by a factor of 100. Only a small fraction of sources in the galactic mid-plane appear to be behind IRDCs, and most of the sources in our final sample of candidate variable stars do not appear to be situated close to any IRDCs. After applying the extinction, we convolved the synthetic spectra with the IRAC 8.0 μ m and MSX 8.28 μ m spectral response curves (see Appendix A of Robitaille et al. 2007 for details of the convolution equations).

Figure 2 show the six synthetic spectra, along with the convolved fluxes. The convolved MSX 8.28 μ m flux does not decrease as fast with increasing A_V as the monochromatic flux at 8.28 μ m. This is because as shown in Figure 1 the spectral response curve for MSX 8.28 μ m actually extends down to 6 μ m (as does IRAC 8.0 μ m) and therefore a large fraction of the flux contributing to the in-band MSX 8.28 μ m flux does not originate from within the region affected by the silicate absorption feature. Even with $A_V=100$, the ratio of IRAC 8.0 μ m to MSX 8.28 μ m only reaches 1.3.

3.3. Combining GLIMPSE I and MSX

We extracted all the MSX point sources from the MSX6C Catalog for which an $8.28\mu\text{m}$ flux was available. We kept only sources for which the uncertainty in the flux values at $8.28\mu\text{m}$ was less than 10% of the flux, and for which the reliability and confusion flags were set to 0 (indicating reliable data). The total number of sources satisfying these criteria and with coordinates in the GLIMPSE I area is 107,091.

In order to avoid the problem of confusion described in the previous section, we decided to use only MSX sources corresponding to a single GLIMPSE source. Specifically, we kept only MSX sources which had exactly one GLIMPSE source within $4''$, and we further required the sum of the IRAC $8.0\mu\text{m}$ flux of neighboring sources within $18''$ to not exceed 20% of the flux of the central GLIMPSE source. In this way, we ensured that we only used MSX sources which corresponded to one GLIMPSE source, with a maximum confusion level of 20%. This reduced the number of sources to consider from 107,091 to 62,013. Note that since the GLIMPSE I Catalog does not include saturated sources as mentioned previously, we are not affected by the apparent variability arising from saturation.

Before looking for true variability, a further criterion was applied. It is possible for sources in IRAC $8.0\mu\text{m}$ to not make it into the GLIMPSE I Catalog, for example, saturated or extended sources, or even diffuse PAH emission. Therefore, even though there may not be bright neighbors *in the Catalog* around a given source, we still need to check that the contamination level is low.

In order to do this, we modified the GLIMPSE I mosaics to match the diffraction-limited and pixel resolutions of MSX: we first smoothed the images using a Gaussian filter so that stars had a half-width at half maximum of $18''$; we then re-binned the mosaics by a factor of five to match the pixel resolution of $6''/\text{pixel}$ of MSX mosaics. The MSX $8.28\mu\text{m}$ mosaics and the IRAC $8.0\mu\text{m}$ mosaics then look very similar. In fact, most stars are seen to have the same relative fluxes in both observations. We then performed PSF fitting photometry on these resampled GLIMPSE I mosaics at the positions of the MSX sources selected above, and compared these fluxes to the fluxes of the matched GLIMPSE point sources found previously. If there was no contamination, one would expect the two fluxes to be very similar. This is the case for many - albeit not all - sources. For this study, we keep only sources for which the original and resampled IRAC $8.0\mu\text{m}$ fluxes do not differ by more than 20%.

Once these criteria were applied, we obtained a list of 50,744 sources. In summary, this list contains sources detected in MSX $8.28\mu\text{m}$, corresponding to a single unsaturated GLIMPSE source, with very little contamination ($< 20\%$) due to confusion, whether from neighboring point sources or other sources of emission. We now use this sample of sources

to search for variability.

3.4. A list of variable star candidates

In light of the results in §3.2, we decided to require the IRAC $8.0\mu\text{m}$ flux from the smoothed GLIMPSE I mosaics and the MSX $8.28\mu\text{m}$ flux to differ by more than a factor of two in order for a source to be considered as potentially variable. This cutoff is conservative since we are aiming for reliability rather than completeness. This reduces the number of sources in the sample from 50,744 to 592. Figure 4 shows the IRAC $8.0\mu\text{m}$ to MSX $8.28\mu\text{m}$ ratio of all 50,744 sources, with the variable star candidates highlighted. We visually inspected the IRAC $8.0\mu\text{m}$ (both original and smoothed) images and residuals, as well as the MSX $8.28\mu\text{m}$ images, in order to check that the photometry was performed correctly in all cases. We eliminated 40 sources where the photometry at $8\mu\text{m}$ on the smoothed mosaics was not reliable (due to confusion or extended emission), further reducing the sample to 552 sources.

These sources are listed in Table 2, along with their respective 2MASS, IRAC and MSX fluxes. In addition to inspecting the IRAC $8.0\mu\text{m}$ and MSX $8.28\mu\text{m}$ images as mentioned above, we examined all the remaining MSX data (bands C, D, and E) using the standard (CB02) and high-sensitivity (CB03) MSX mosaics. We eliminated any unreliable fluxes where the corresponding source was very noisy or absent from the images, since we use the data in these bands for further source selection (§4.1) and when plotting the SEDs. Therefore we can rule out bad data and unreliable photometry as a cause of apparent variability. We have also included MIPS $24.0\mu\text{m}$ fluxes when data were available, as described in the next section.

Although we cannot rule out that strong spectral features around $10\mu\text{m}$ or at $6\text{--}6.5\mu\text{m}$ are causing offsets by more than a factor of two between IRAC $8.0\mu\text{m}$ and MSX $8.28\mu\text{m}$, we see from the results in §3.2 that such spectral variations cannot be explained by thermal dust spectrum with a silicate feature or a standard extinction law. Therefore, even if the sources in this sample are not all intrinsically variable, they remain very interesting objects for future follow-up studies.

4. Highly likely variable star candidates

4.1. Source selection

In this section, we use the sample of 552 sources to search for a subset which present secondary indicators of variability. To do this, we use several criteria:

Very high variability We flag a source as highly likely to be variable if the fluxes at IRAC $8.0\mu\text{m}$ and MSX $8.28\mu\text{m}$ differ by more than a factor of 4. It is extremely difficult to explain how such a flux could be due to strong spectral features, and we can rule out problems associated with the data, as we have visually quality-checked all the IRAC and MSX data used. Using this selection criterion, we find 11 sources.

JHK_s/IRAC mismatch If a star is truly variable and presents a large difference (e.g. a factor of two difference) in flux at $8\mu\text{m}$, it is reasonable to assume that in some cases at least, the source should also be variable at shorter wavelengths. Since the 2MASS and IRAC data were taken a few years apart, we can therefore search for an apparent mismatch between JHK_s and IRAC fluxes. However, since these two wavelength ranges do not overlap, it is not straightforward to do this, and we restrict ourselves to cases where the mismatch is the most obvious.

We decided to remove sources with JHK_s and IRAC data consistent with the colors of stars or YSOs with no variability. This includes sources with colors consistent with those of AGB stars with no variability, since AGB stars are known to have IRAC colors similar to those of YSOs (as can be seen by comparing the color-color diagrams in Robitaille et al. 2006 and Marengo et al. 2006).

In order to do this, we use the SED fitting tool described in Robitaille et al. (2007), to which we have added the grid of stellar photosphere models from Castelli & Kurucz (2004). The fitting tool uses linear regression to fit model stellar and YSO SEDs to observed SEDs, allowing the interstellar extinction and the distance to be free parameters.

We first fit all the sources, using only JHK_s and IRAC data, with the stellar photosphere models, and allowing a range of A_V from 0 to 30. We then consider all sources fit with a χ^2 per datapoint of less than 2 as being consistent with no mismatch. The cutoff value is arbitrary, but visual inspection shows that all fits with a smaller χ^2 per datapoint are very good. We then fit the remaining sources with YSO models, again considering all sources with a χ^2 per datapoint of less than 2 as being consistent with no mismatch. We assumed that the objects could lie anywhere from 300 pc to 10 kpc, with an interstellar A_V of up to

40. Out of the 552 sources in our list of variable star candidates, 496 had enough data to be used in the SED fitting tool (we required data for at least four wavelengths from JHK_s and IRAC); 78 were well fit by stellar photosphere models and 391 were well fit by YSO models, leaving 27 sources. These sources were in some cases badly fit for reasons other than a JHK_s/IRAC mismatch, so after visual inspection of the SEDs we selected a sample of 15 sources for which an offset in the SED between JHK_s and IRAC was clearly the cause of the bad fit.

A mismatch between JHK_s and IRAC could be due to a high K_s-band flux which can in turn be due to the confusion in the K_s-band (this would occur more frequently at longitudes towards the inner galaxy). Therefore, we visually inspected the JHK_s and IRAC images for this subset of sources in order to ensure that this was not the case, and ruled this out for the 15 sources.

We can of course not rule out that the offset between 2MASS and IRAC is simply due to intrinsically exotic SEDs for these sources (e.g. due to near-IR spectral lines or multiple sources) but it seems likely that in most cases, variability is the main cause of offset, especially when considered alongside the fact that the IRAC 8.0 μ m and MSX 8.28 μ m fluxes are also offset from each other by at least a factor of two.

In order to illustrate the above procedure, we show the SEDs of three sources in Figure 5 with the best model SED fit in each case. These include a source well explained by a stellar photosphere model, a source well explained by a YSO model, and a source for which we could not fit any models well due to the offset between JHK_s and IRAC.

MSX 21.3 μ m and MIPS 24.0 μ m mismatch Finally, we flag sources as being likely variables if there is a clear offset between the MIPS 24.0 μ m and the MSX 21.3 μ m flux. We measured the MIPS 24.0 μ m fluxes using PSF photometry on data available in the Spitzer Science Center Archive (MIPSGAL Program; PI Carey) for the 552 sources in the sample using a custom written PSF fitting program. Since we can ignore saturated pixels in the fitting, we are able to extract fluxes up to 2-3 Jy for mildly saturated sources. As for MSX 8.28 μ m and IRAC 8.0 μ m, we have to be careful when looking for offsets between MIPS 24.0 μ m and MSX 21.3 μ m fluxes because of the difference in wavelength and spectral response (see Figure 1). We performed an analysis - similar to that described in §3.2 - for MSX 21.3 μ m and MIPS 24.0 μ m, and found that although ratios of MIPS 24.0 μ m/MSX 21.3 μ m larger than 2 are possible, due to steeply rising dust spectra at those wavelengths, ratios less than 0.5 cannot be reproduced by the models (see right-hand panel of Figure 3). Therefore, we select only sources where MIPS 24.0 μ m/MSX 21.3 μ m < 0.5. As mentioned previously, the MSX images for all bands were checked visually, and the band E fluxes for

the sources in our sample are reliable. Using this criterion, we find 14 sources. These are highlighted in the right-hand panel of Figure 4.

Table 4 lists the 40 sources in our sample of 552 which satisfy at least one of the above three criteria. The SEDs for all 40 sources are presented in Figures 6, 7, and 8.

4.2. Typical examples

In Figure 9, we show a selection of images for three sources, one from each of the above sub-samples in turn, as well as the SED for these sources. The sources are:

G337.0848–00.5550 This source (shown in the left panels) has a ratio of IRAC $8.0\mu\text{m}$ to MSX $8.28\mu\text{m}$ of 0.23, and therefore is flagged as an ‘extreme variable’. The large variability is clearly seen by comparing the IRAC $8.0\mu\text{m}$ and MSX $8.28\mu\text{m}$ images. This source also shows a possible JHK_s mismatch, but the offset was not large enough to make it through our selection process. However, in the light of the extreme variability in IRAC $8.0\mu\text{m}$, it seems likely that the offset between JHK_s and IRAC wavelengths is real. There is no possible source of confusion at K_s and $3.6\mu\text{m}$, as shown in the images.

G346.1049–00.4608 The MIPS $24.0\mu\text{m}$ and MSX $21.3\mu\text{m}$ fluxes for this source (shown in the center panels) differ by more than a factor of two. The top two panels show the difference between the source brightness in IRAC $8.0\mu\text{m}$ and MSX $8.28\mu\text{m}$, whereas the two panels below show the difference between MIPS $24.0\mu\text{m}$ and MSX $21.3\mu\text{m}$. The difference is more difficult to see in the latter due to the high noise in the MSX $21.3\mu\text{m}$ mosaic. However, whereas the central source is slightly brighter than the source shown in the top right in MSX $21.3\mu\text{m}$, the two sources have a more similar flux in MIPS $24.0\mu\text{m}$. A very interesting source is present to the bottom right - G346.0803–00.4808. It is brighter than G346.1049–00.4608 in MIPS $24.0\mu\text{m}$, yet is undetected in MSX $21.3\mu\text{m}$! Unfortunately it is not present in our sample of 552 sources, because its IRAC flux lies less than 5% above the ‘mild saturation’ limit.

G318.9134+00.7526 This source (shown in the right panels) shows a very large offset between JHK_s and IRAC, and this is clearly not due to any issues with the matching of the 2MASS to the GLIMPSE source after inspection of the images. In fact, the offset in the SED is so large that the slope from K_s to $3.6\mu\text{m}$ is actually bluer than for a normal star. This can be seen in the two top panels - the central star actually becomes fainter relative to all the

surrounding stars from K_s to $3.6\mu\text{m}$. As shown in the two panels below, the brightness of the source then increases significantly between IRAC $8.0\mu\text{m}$ and MSX $8.28\mu\text{m}$. This source is probably our best candidate in the overall sample.

5. Analysis and Discussion

5.1. Possible mechanisms of mid-IR variability

We now discuss the main mechanisms for variability in the mid-IR. The types of sources that are likely to show such variability are the following:

Asymptotic Giant Branch (AGB) stars Long Period Variables (LPVs; classified into Mira, semiregular, and slow irregular variables), which are known to be AGB stars, show variability by factors of hundreds or thousands in the optical over timescales of months to years. These low- to intermediate-mass stars which are undergoing shell Helium fusion suffer large mass losses through stellar winds, and are thought to be one of the main dust production sites in the Galaxy. The dust chemistry can either be carbon or oxygen dominated, which leads to the two types of AGB stars being referred to as Carbon- or Oxygen-rich. A third type of AGB stars has been observed, with very red near-IR colors; these are referred to “extreme” AGB stars (e.g. Blum et al. 2006), the brightest of which were previously identified as “obscured” AGB stars (e.g. Loup et al. 1997). These are mostly C-rich AGB stars with large amounts of circumstellar dust.

Optical to mid-IR studies of Mira variables have shown that the amplitude of the variability generally decreases with wavelength (Lockwood & Wing 1971; Le Bertre 1992, 1993; Barthes et al. 1996; Smith et al. 2002), with the exception of the silicate feature around $10\mu\text{m}$, where the amplitude of the variations is higher than at immediately smaller and larger wavelengths (Le Bertre 1993). Little-Marenin et al. (1996) also show that the strength of the silicate feature in AU Cygni (an O-rich AGB star) varies with time.

Key signatures of variability due to AGB stars are therefore the presence of a thermal IR excess, a decrease in the amplitude of the variations with wavelength, and a silicate feature with varying strength.

Pre-main-sequence stars Optical and UV variability is common in pre-main-sequence stars. T Tauri stars for example are variable by definition (Joy 1945); the variability in these objects has been attributed to hot and cool spots on the stellar surface, the former due to

magnetospheric accretion, and the latter (also referred to as starspots) due to inhibition of the convection by a strong magnetic field. At longer wavelengths, where the bulk of the flux is due to thermal emission from the dust, variability is somewhat less common. However, various types of pre-main-sequence stars show infrared variability, including Herbig Ae/Be stars (Prusti & Mitskevich 1994), FU Ori type objects (Ábrahám et al. 2004), and UX Ori type objects (Juhász et al. 2007).

Key signatures of pre-main-sequence stars include the presence of a thermal IR excess, and the presence of a silicate feature at 10 microns (whether in absorption or emission). These are a priori indistinguishable from the signatures expected for AGB stars. However, an additional signature which is specific to YSOs would be the large-scale spatial correlation of variables in our sample with known star-formation regions.

Active Galactic Nuclei (AGNs) Variability has been observed in AGNs on timescales of hours to years, and at X-ray, UV, optical, infrared, and radio wavelengths. In the mid- and far-infrared, evidence suggests that blazars, including BL Lac objects, are the most variable AGNs, while Seyfert 1 & 2 galaxies and quasars are less variable (e.g. Edelson & Malkan 1987; Sembay et al. 1987).

A key signature of AGNs would be a relatively uniform distribution in the plane of the sky, with no correlation with the distribution of Galactic sources.

5.2. Physical nature of the variable star candidates

In order to determine whether the sources are most likely to be galactic (e.g. AGBs or YSOs) or extra-galactic (e.g. AGNs), we examine the spatial distribution of the sources in our list of variable star candidates. Figure 10 shows the galactic longitude and latitude distribution of the 552 variable star candidates, as well as their spatial distribution. The number of variable sources clearly peaks towards the galactic center (~ 6 /square degree at $|\ell| = 10^\circ$), and tends to very low values (< 1 /square degree at $|\ell| = 65^\circ$) further away from the center. This indicates that the large majority of the sources are galactic. If the sources were extragalactic, one should not observe any increase in source density towards the galactic center. In fact, one would expect a *decrease* towards the galactic center due to the increased line-of-sight extinction through the galaxy. The latitude distribution is consistent with a flat distribution, but we note that this may simply be because we only extend out to $b = \pm 1^\circ$

The Galactic distribution of the variable star candidates does not correlate strongly

with the location of massive star formation regions (e.g. M16 at $(\ell, b) \approx (15^\circ, -0.7^\circ)$, M17 at $(\ell, b) \approx (17^\circ, 0.8^\circ)$, or the G305 complex at $(\ell, b) \approx (305.2^\circ, 0.1^\circ)$), suggesting that the majority of sources are likely to be AGBs rather than YSOs.

Based purely on the Galactic longitude distribution of the sources, we can rule out extragalactic sources of variability such as AGNs for the vast majority of sources, and based on the spatial distribution, we favor the AGB interpretation.

In Figure 11 we show the JHK_s colors of all the sources in the sample of 552 for which fluxes in J, H, and K_s bands were available, as well as the IRAC colors for all sources for which fluxes in all IRAC bands were available. The sources shown are clearly much redder than un-obscured stars. We show the locus for reddened photospheres in the JHK color-color plot, and the range of expected colors for YSOs in the IRAC color-color plot (adapted from Robitaille et al. 2006). Both the red H-K color and the IRAC colors of these sources suggests the presence of thermal dust emission, in agreement with both the YSO and the AGB interpretation.

Finally, we mention that a few sources in Figure 8 show a wavelength-dependence for the variability. For example, G318.9134+00.7526 (also shown in Figure 9) and G035.8416+00.5887 both display a very large offset between K_s and IRAC 3.6 μ m (at least an order of magnitude), whereas the offset at 8 μ m is somewhat smaller (half an order of magnitude). This is what one would expect if these were AGB stars/Mira variables.

5.3. Comparison to known sources

We searched for the 552 sources from our list of variable star candidates in the Combined General Catalogue of Variable Stars (GCVS4.2; Samus & Durlevich 2004) - which lists 430 sources in the GLIMPSE I survey area - and found that none are listed as known or suspected variable stars. This is expected, as most of these are likely to be too extinguished to be seen at optical wavelengths.

One of the sources in the sub-sample of 40, G338.2051–00.3526, was found to match with a source in the ISOGAL survey classified as a YSO (ISOGAL-P J164144.9-465006; Felli et al. 2002).

We then compared our list of sources - before and after selection - to the IRAS Point-Source Catalog in order to verify whether our selection procedure increased the fraction of sources with high variability probability (the `Var` index). We searched for the 50,744 sources used for the initial selection of variable sources in the IRAS Point-Source Catalog, and found

3,292 with an IRAS source within $15''$. Of the 552 variable candidates, 95 have a corresponding IRAS source, and of the 40 highly likely variable sources, 15 have a corresponding IRAS source. In Table 3 we list in each case the fraction of IRAS sources with a **Var** index of at least 95%. We found that the initial selection of variable stars increased the fraction of IRAS sources with **Var** > 95% from 7.7% to 27.4%, and the further selection of candidates with a secondary indicator of variability increased the fraction further to 46.6%.

We repeated this analysis by using the **var** flags from the MSX Point-Source Catalog (available for all sources, since all the sources in our lists originate from the MSX Point-Source Catalog). The results are also shown in Table 3. The initial selection of variable sources increases the number of sources with the variability flag set in at least one band from 17.3% to 42.8%. When considering sources with at least two variability flags set, the fraction increases from 1.0% to 6.3% when selecting the 552 variable stars, and the refinement of the sample to 40 sources increases this to 12.5%.

The above results indicate that one quarter to half of the sources in the list of 552 variable star candidates, and at least 40% of the sub-sample of 40 are likely to be variable on timescales of months, i.e. the time between the multiple IRAS or MSX observations. If the remaining sources in our sample of 552 are truly variable, this suggests that the timescales of their variability has to be larger than the lifetime of the MSX and IRAS missions, and therefore has to be of the order of years. We have included both the **Var** index and $\sum \text{var}$ (the sum of the variability flags) for each source in Table 2.

Finally, we searched the original Dutch Low Resolution Spectrograph (LRS) database in order to find mid-IR spectra for the sub-sample of 40 sources. Three sources were found to have LRS spectra, two of which were extremely noisy. The third, G296.6843+00.4515 (IRAS 11557-6129), shows a dominant broad $10\mu\text{m}$ emission feature. Its width, peak, and shape all suggest the presence of O-rich dust in the form of amorphous silicates. This is shown in the right hand panel of Figure 12. The data shown are in fact the ‘Average’² of three LRS spectra taken at different epochs, ranging over 43 days (27th July, 5th August, and 9th September 1983). We extracted the individual spectra for the three epochs, and have shown these in Figure 12. Despite the noise in the data, it does appear that: (1) the strength of the silicate feature changes over the three epochs, and (2) the continuum level also changes (as seen from the monochromatic flux at $8\mu\text{m}$). These signatures suggest that this source is indeed an O-rich AGB star displaying variability.

²As defined in the IRAS Explanatory Supplement, Chapter IX.C.3

6. Conclusion

We have selected a sample of 552 sources for which the IRAC $8.0\mu\text{m}$ and MSX $8.28\mu\text{m}$ flux differ by more than a factor of two. We have checked that the data are of sufficient quality through selection criteria and visual inspection of the data for all these sources. We have ruled out that differences of more than a factor of two can be due to the silicate feature in a standard interstellar extinction law, or silicates seen in absorption or emission in YSOs using standard models. Therefore, this sample contains objects which are all potentially interesting for follow-up observations, even if not variable, as they may show a deviation from standard extinction, different emission processes in YSOs (such as PAH emission), or other strong spectral features in YSOs and AGB stars. If most of these sources are confirmed as variable, they will significantly expand the number of known variable stars in the Galactic plane: as mentioned in §5.3, the GCVS v4.2 only lists 430 sources in the GLIMPSE I survey area.

We further refined this sample to a subset of sources for which a secondary indicator of variability was available. We selected sources for which the variability at $8\mu\text{m}$ is very strong, with IRAC $8.0\mu\text{m}$ and MSX $8.28\mu\text{m}$ differing by more than a factor of four. We also selected sources for which the MIPS $24.0\mu\text{m}$ to MSX $21.3\mu\text{m}$ ratio was less than half, and finally we selected sources for which the JHK_s and IRAC data appear to be offset. The number of sources in each category is 11, 14, and 15 respectively.

By comparing the lists of sources before and after selection with the `Var` index in the IRAS Point-Source Catalog and the `var` flags in the MSX Point-Source Catalog, we estimate that at least one quarter to half of sources in the sample of 552 sources are truly variable, on timescales up to months. The remaining sources are either truly variable, albeit on longer timescales (years), or contain strong spectral features which cause the offset between the IRAC $8.0\mu\text{m}$ and the MSX $8.28\mu\text{m}$ flux.

We have also presented multi-epoch IRAS LRS spectra which tentatively confirm variability in one of the sources (G296.6843+00.4515), and show a silicate feature varying in strength over time, suggesting that this sources is an O-rich AGB star.

The analysis we have performed is a preliminary selection of the most prominent candidate variables, and by no means a complete census of mid-IR variability in the Galaxy. We are biased towards bright sources in GLIMPSE and faint sources in MSX. Since we require sources to be unsaturated in GLIMPSE and detected in MSX, we are biased towards objects with redder spectral slopes. In addition, when searching for MSX $21.3\mu\text{m}$ and MIPS $24.0\mu\text{m}$ mismatches, or JHK_s and IRAC offsets, we are biasing the sample further towards objects with redder slopes, because the sensitivity in MSX $21.3\mu\text{m}$ is even lower than MSX

8.28 μ m. Despite all these restrictions, we find 552 sources with IRAC 8.0 μ m and MSX 8.28 μ m fluxes differing by at least a factor of two, and 40 sources with secondary evidence for variability.

While we were restricted to using $\sim 50,000$ sources that were in common between GLIMPSE I and MSX and not affected by confusion, the total number of Catalog sources in the GLIMPSE I survey is around 31,000,000. This suggests that our sample is really just a very small tip of the Galactic iceberg, and that the true number of variable sources is very likely to be of the order of tens of thousands.

We wish to thank the anonymous referee, and Bob Benjamin, for useful suggestions. This research made use of data products from the Midcourse Space Experiment; the NASA/IPAC Infrared Science Archive, which is operated by the Jet Propulsion Laboratory, California Institute of Technology, under contract with the National Aeronautics and Space Administration; and the Vizier service (Ochsenbein et al. 2000). Partial support for this work was provided by a Scottish Universities Physics Alliance Studentship (TR). MC thanks NASA for supporting his participation in this work through contract 1242593 with the University of California, Berkeley. Additional support, as part of the Spitzer Space Telescope Theoretical Research Program (BW, TR), Legacy Science Program (EC, MM, BB, BW), and Fellowship Program (RI), was provided by NASA through contracts issued by the Jet Propulsion Laboratory, California Institute of Technology under a contract with NASA.

REFERENCES

- Ábrahám, P., Kóspál, Á., Csizmadia, S., Kun, M., Moór, A., & Prusti, T. 2004, *A&A*, 428, 89
- Barthes, D., Chenevez, J., & Mattei, J. A. 1996, *AJ*, 111, 2391
- Benjamin, R. A. et al. 2003, *PASP*, 115, 953
- Blum, R. D. et al. 2006, *AJ*, 132, 2034
- Cardelli, J. A., Clayton, G. C., & Mathis, J. S. 1989, *ApJ*, 345, 245
- Castelli, F., & Kurucz, R. L. 2004, *ArXiv Astrophysics e-prints*
- Cohen, M., Wheaton, W. A., & Megeath, S. T. 2003, *AJ*, 126, 1090
- Cohen, M., Witteborn, F. C., Walker, R. G., Bregman, J. D., & Wooden, D. H. 1995, *AJ*, 110, 275

- Edelson, R. A., & Malkan, M. A. 1987, *ApJ*, 323, 516
- Egan, M. P. et al. 2003, *VizieR Online Data Catalog*, 5114, 0
- Engelbracht, C. W. et al. 2007, *ArXiv e-prints*, 704
- Fazio, G. G. et al. 2004, *ApJS*, 154, 10
- Felli, M., Testi, L., Schuller, F., & Omont, A. 2002, *A&A*, 392, 971
- Flaherty, K. M., Pipher, J. L., Megeath, S. T., Winston, E. M., Gutermuth, R. A., Muzerolle, J., Allen, L. E., & Fazio, G. G. 2007, *ApJ*, 663, 1069
- Joy, A. H. 1945, *ApJ*, 102, 168
- Juhász, A., Prusti, T., Ábrahám, P., & Dullemond, C. P. 2007, *MNRAS*, 374, 1242
- Le Bertre, T. 1992, *A&AS*, 94, 377
- . 1993, *A&AS*, 97, 729
- Little-Marenin, I. R., Stencel, R. E., & Staley, S. B. 1996, *ApJ*, 467, 806
- Lockwood, G. W., & Wing, R. F. 1971, *ApJ*, 169, 63
- Loup, C., Zijlstra, A. A., Waters, L. B. F. M., & Groenewegen, M. A. T. 1997, *A&AS*, 125, 419
- Marengo, M., Hora, J. L., Barmby, P., Willner, S. P., Allen, L. E., Schuster, M. T., & Fazio, G. G. 2006, *ArXiv Astrophysics e-prints*
- Ochsenbein, F., Bauer, P., & Marcout, J. 2000, *A&AS*, 143, 23
- Price, S. D., Egan, M. P., Carey, S. J., Mizuno, D. R., & Kuchar, T. A. 2001, *AJ*, 121, 2819
- Price, S. D., Paxson, C., Engelke, C., & Murdock, T. L. 2004, *AJ*, 128, 889
- Prusti, T., & Mitskevich, A. S. 1994, in *Astronomical Society of the Pacific Conference Series*, Vol. 62, *The Nature and Evolutionary Status of Herbig Ae/Be Stars*, ed. P. S. The, M. R. Perez, & E. P. J. van den Heuvel, 257–+
- Reach, W. T. et al. 2005, *PASP*, 117, 978
- Rieke, G. H. et al. 2004, *ApJS*, 154, 25
- Robitaille, T. P., Whitney, B. A., Indebetouw, R., & Wood, K. 2007, *ApJS*, 169, 328

- Robitaille, T. P., Whitney, B. A., Indebetouw, R., Wood, K., & Denzmore, P. 2006, *ApJS*, 167, 256
- Samus, N. N., & Durlevich, O. V. 2004, *VizieR Online Data Catalog*, 2250, 0
- Sembay, S., Hanson, C. G., & Coe, M. J. 1987, *MNRAS*, 226, 137
- Skrutskie, M. F. et al. 2006, *AJ*, 131, 1163
- Smith, B. J., Leisawitz, D., Castelaz, M. W., & Luttermoser, D. 2002, *AJ*, 123, 948
- Spear, G. G., Owen, B., & Madore, B. 1993, in *Astronomical Society of the Pacific Conference Series*, Vol. 43, *Sky Surveys. Protostars to Protogalaxies*, ed. B. T. Soifer, 35–+
- Tsuji, T. 2001, *A&A*, 376, L1
- Tsuji, T. 2003, in *ESA Special Publication*, Vol. 511, *ESA Special Publication*, ed. C. Gry, S. Peschke, J. Matagne, P. Garcia-Lario, R. Lorente, & A. Salama, 93–+
- Werner, M. W. et al. 2004, *ApJS*, 154, 1

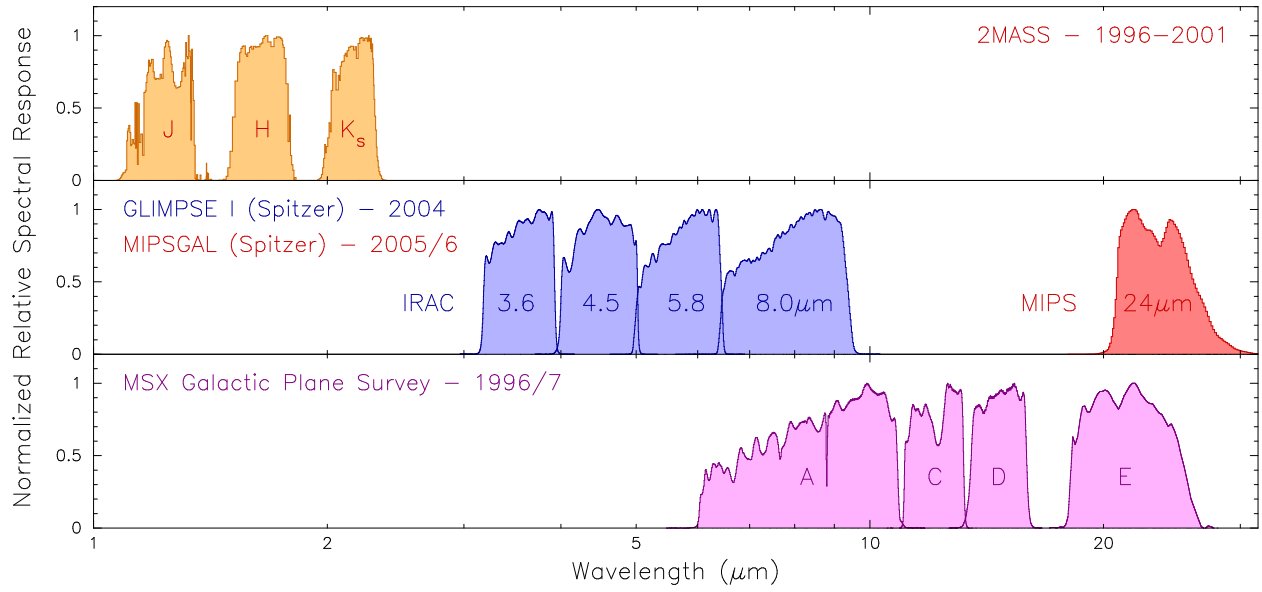


Fig. 1.— The spectral response curves for 2MASS JHK_s, *Spitzer* IRAC and MIPS 24.0 μm , and MSX. Note that there is significant overlap between the IRAC 8.0 μm and MSX 8.28 μm filters, and between the MSX 21.3 μm and MIPS 24.0 μm filters.

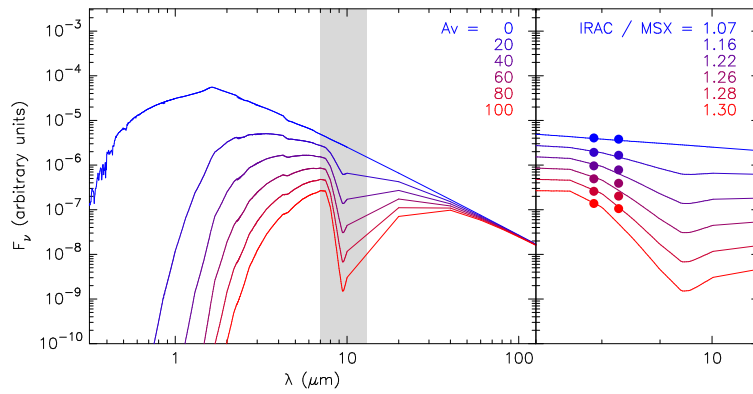


Fig. 2.— The spectrum of a 4,000 K star for values of the visual extinction A_V ranging from 0 to 100 (top to bottom spectra). The region indicated by the gray area in the left panel is shown in more detailed in the right panel. The points show the synthetic fluxes for IRAC $8.0 \mu\text{m}$ and MSX $8.28 \mu\text{m}$. The ratio of the IRAC $8.0 \mu\text{m}$ to the MSX $8.28 \mu\text{m}$ flux for each spectrum is given in the right panel.

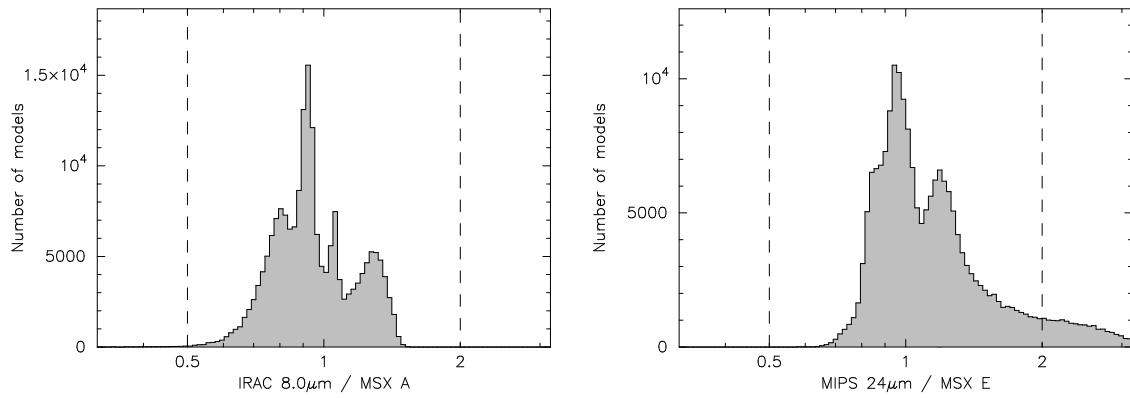


Fig. 3.— Calculated ratios of the IRAC $8.0\mu\text{m}$ fluxes to the MSX $8.28\mu\text{m}$ fluxes (left) and of the MIPS $24.0\mu\text{m}$ fluxes to the MSX $21.3\mu\text{m}$ fluxes (right) for the grid of YSO model SEDs presented in Robitaille et al. (2006). The vertical lines delimit in each case the region within which the two fluxes agree to within a factor of two. The peaks in both distributions are artifacts due to the sampling of parameter space for the model grid (see Robitaille et al. for more details on the sampling of the parameters).

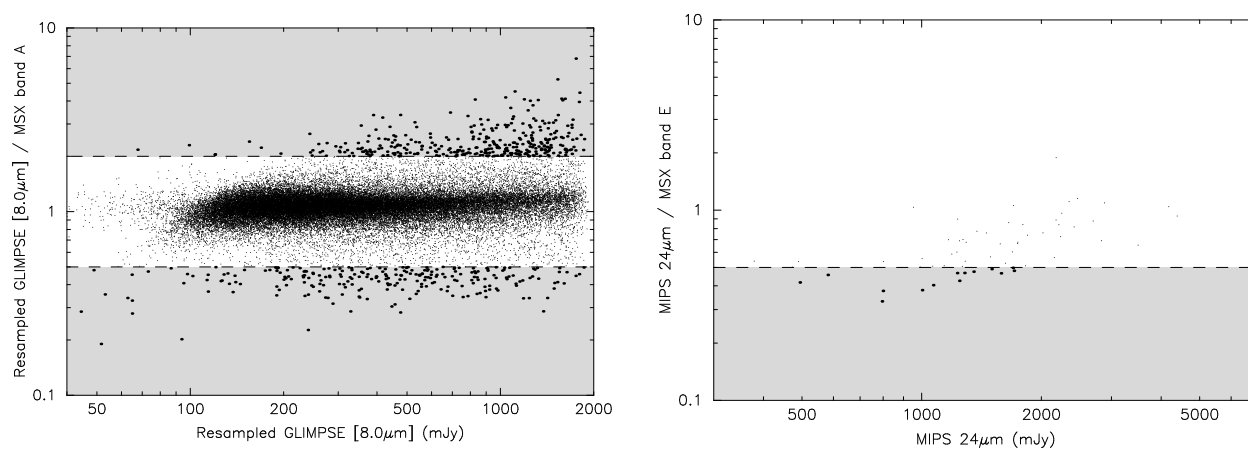


Fig. 4.— Left: ratio of the IRAC $8.0\mu\text{m}$ to the MSX $8.28\mu\text{m}$ fluxes for all sources for which the IRAC $8.0\mu\text{m}$ flux from the GLIMPSE Catalog and from the smoothed mosaics agree to within 20%. The dashed lines indicate where the ratios are equal to 0.5 and 2, and the grey areas show the regions within which we flag sources as variable. Right: ratio of the MIPS $24.0\mu\text{m}$ to the MSX $21.3\mu\text{m}$ fluxes for all sources from the sample of 552 sources for which both fluxes were available. Similarly to the left panel, the dashed line indicates where the ratios are equal to 0.5, and the gray areas show the regions within which we flag sources as variable.

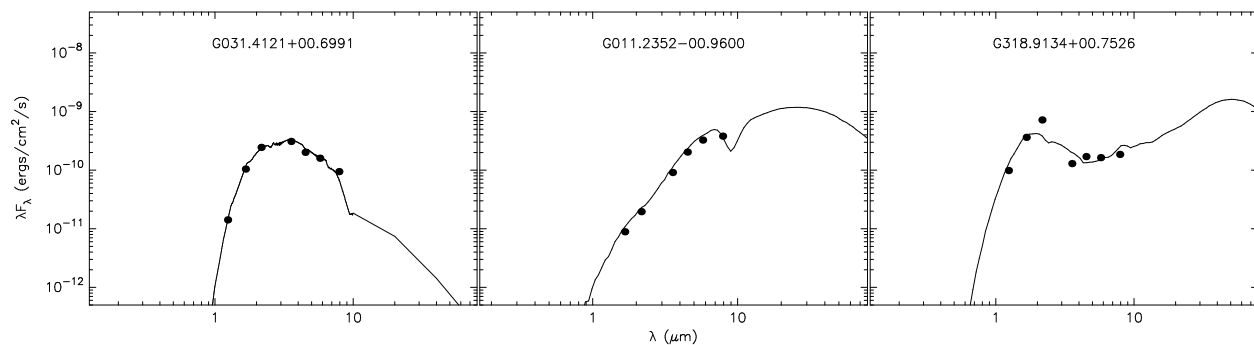


Fig. 5.— Model SED fits to the broadband photometry of three example sources to find offsets between JHK_s and IRAC data. The data are shown as points and the models as solid lines. The error bars are smaller than the points. Left: a source whose data are consistent with a reddened stellar photosphere. Center: a source whose data are consistent with a model SED for an embedded protostar. Right: a source that is not well fit by model SEDs for stars or YSOs. The cause of the bad fit is the mismatch between the JHK_s and IRAC points. The model shown is the best fit obtained with YSO models.

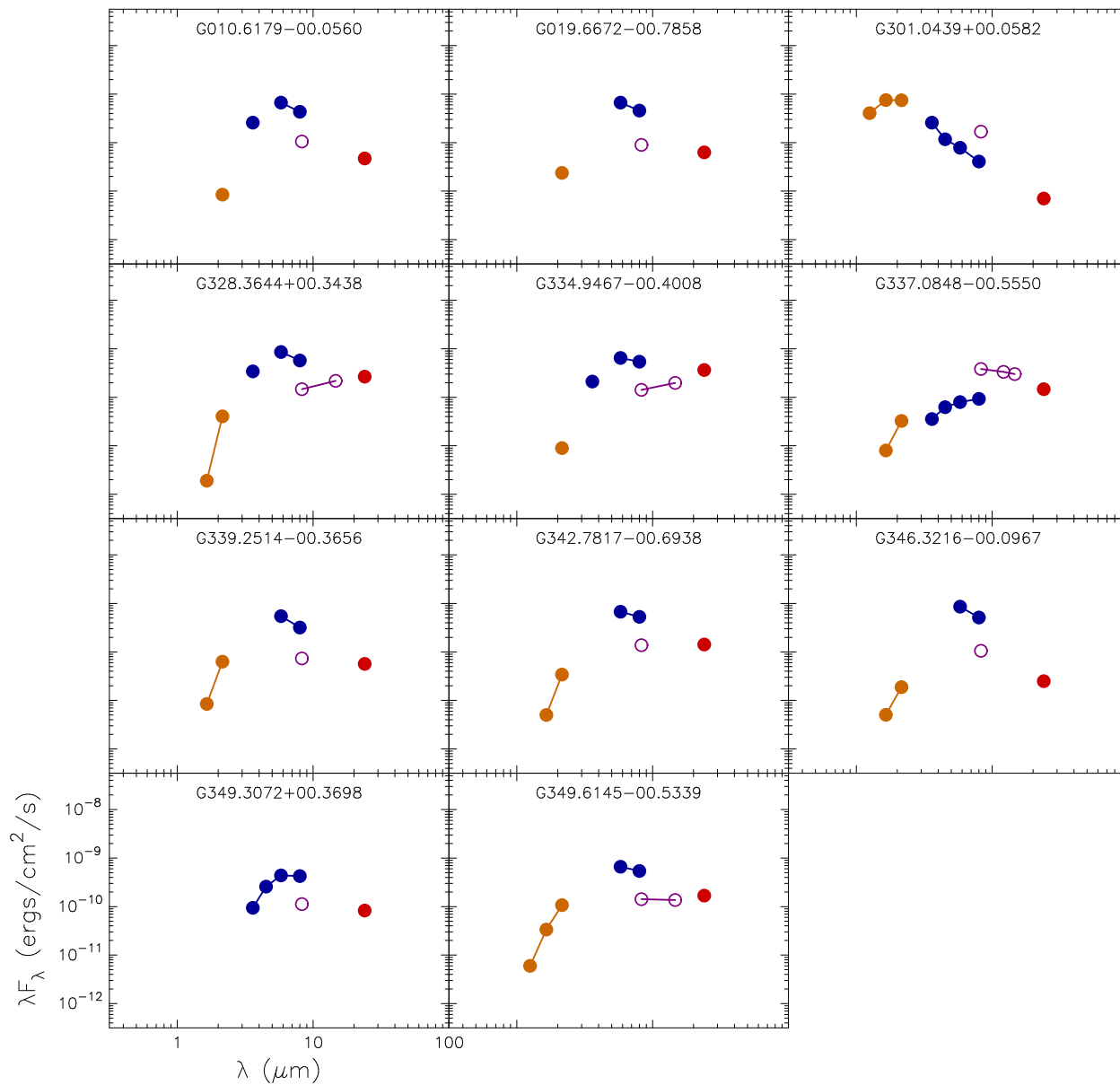


Fig. 6.— The SEDs for the sources where IRAC 8.0 μ m and MSX 8.28 μ m differ by more than a factor of four. The filled circles show (when available), from left to right, 2MASS, IRAC, and MIPS 24.0 μ m data points. The open circles show (when available) the MSX data points.

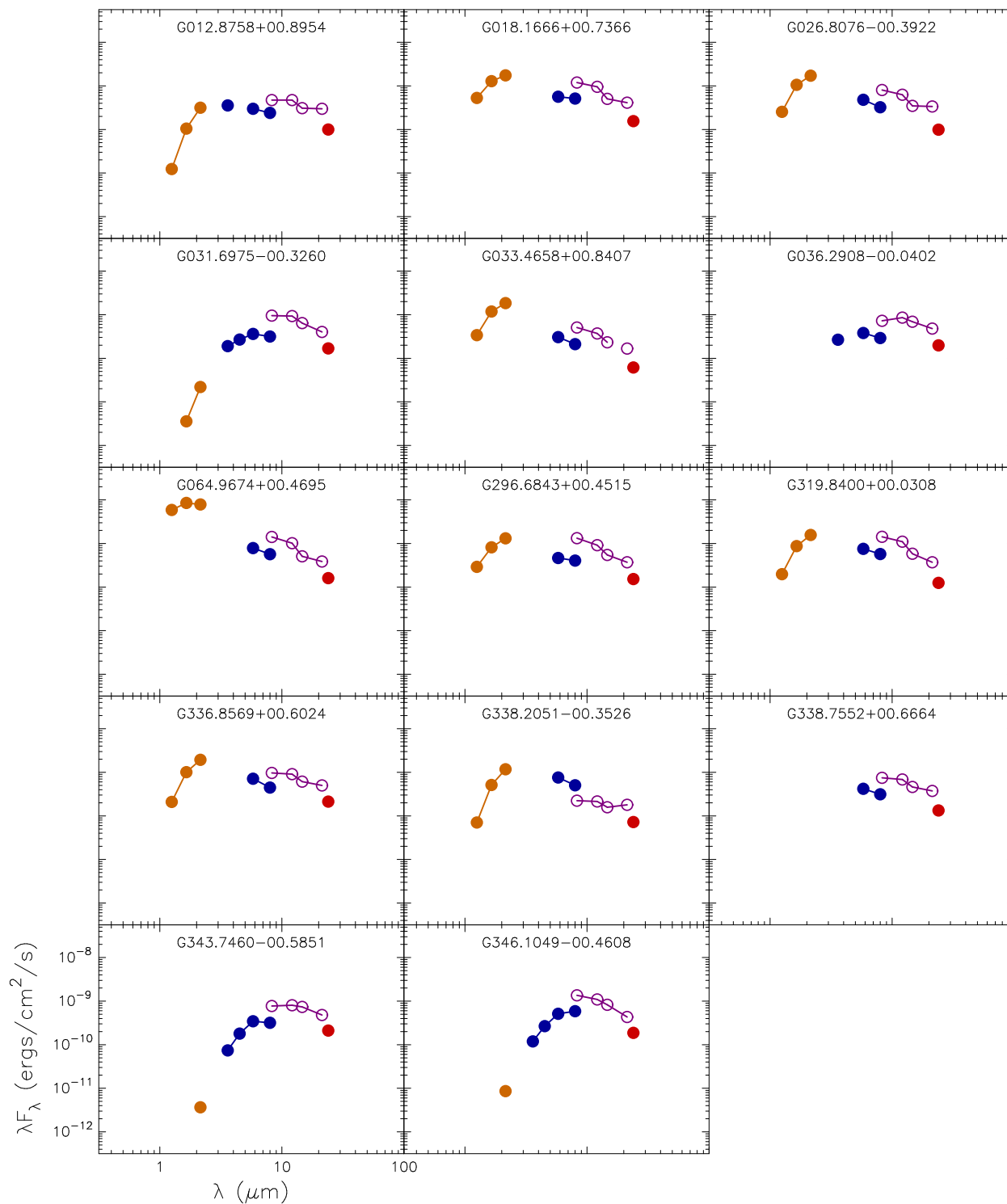


Fig. 7.— The SEDs for the sources where in addition to the IRAC $8.0\mu\text{m}$ and MSX $8.28\mu\text{m}$ fluxes differing by more than a factor of two, the MSX $21.3\mu\text{m}$ and MIPS $24.0\mu\text{m}$ fluxes also differ by more than a factor of two. The data points follow the same style as in Figure 6. .

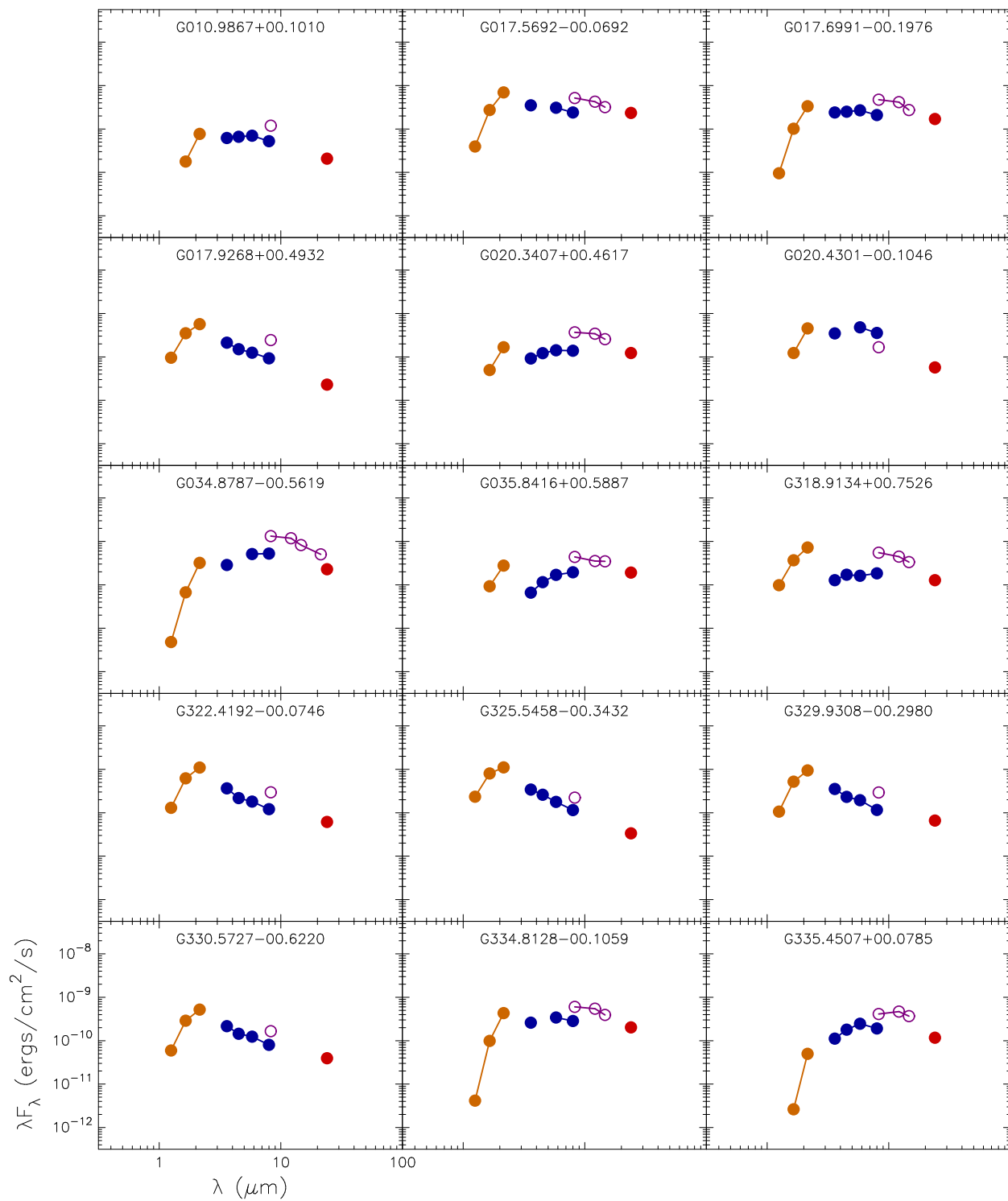


Fig. 8.— The SEDs for the sources where in addition to the IRAC $8.0\mu\text{m}$ and MSX $8.28\mu\text{m}$ fluxes differing by more than a factor of two, the JHK_s and IRAC data seem to be offset. The data points follow the same style as in Figure 6.

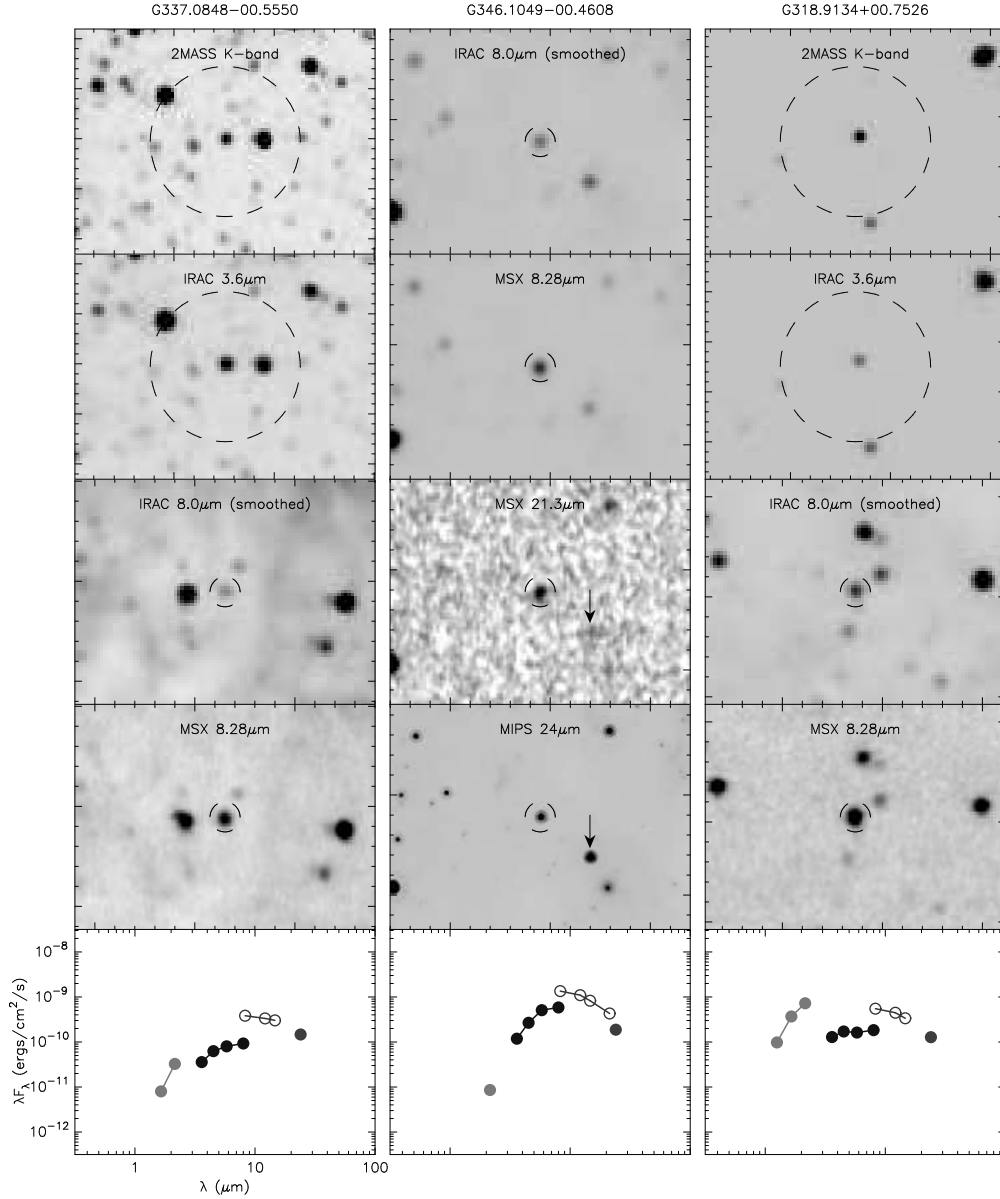


Fig. 9.— Images for three sources. For each source, four images are shown, and the bottom panel shows the SED. The IRAC 3.6 μm images are slightly smoothed to match the 2MASS resolution. The circles in each plot are 27'' in radius (the K and IRAC 3.6 μm images are shown on a smaller scale). The arrow indicates G346.0803-00.4808, which did not make it to our sample of variable stars (as it is very mildly saturated in IRAC), but appears to be highly variable in MSX 21.3 μm and MIPS 24.0 μm (the flux differs by a factor of at least ~2.5). The K_s and IRAC 3.6 μm plots for G318.9134+00.7526 are shown on a different stretch to show that the slope of the SED is bluer between K_s and IRAC 3.6 μm than the surrounding stars. The three SEDs are presented in the same way as in Appendix A.

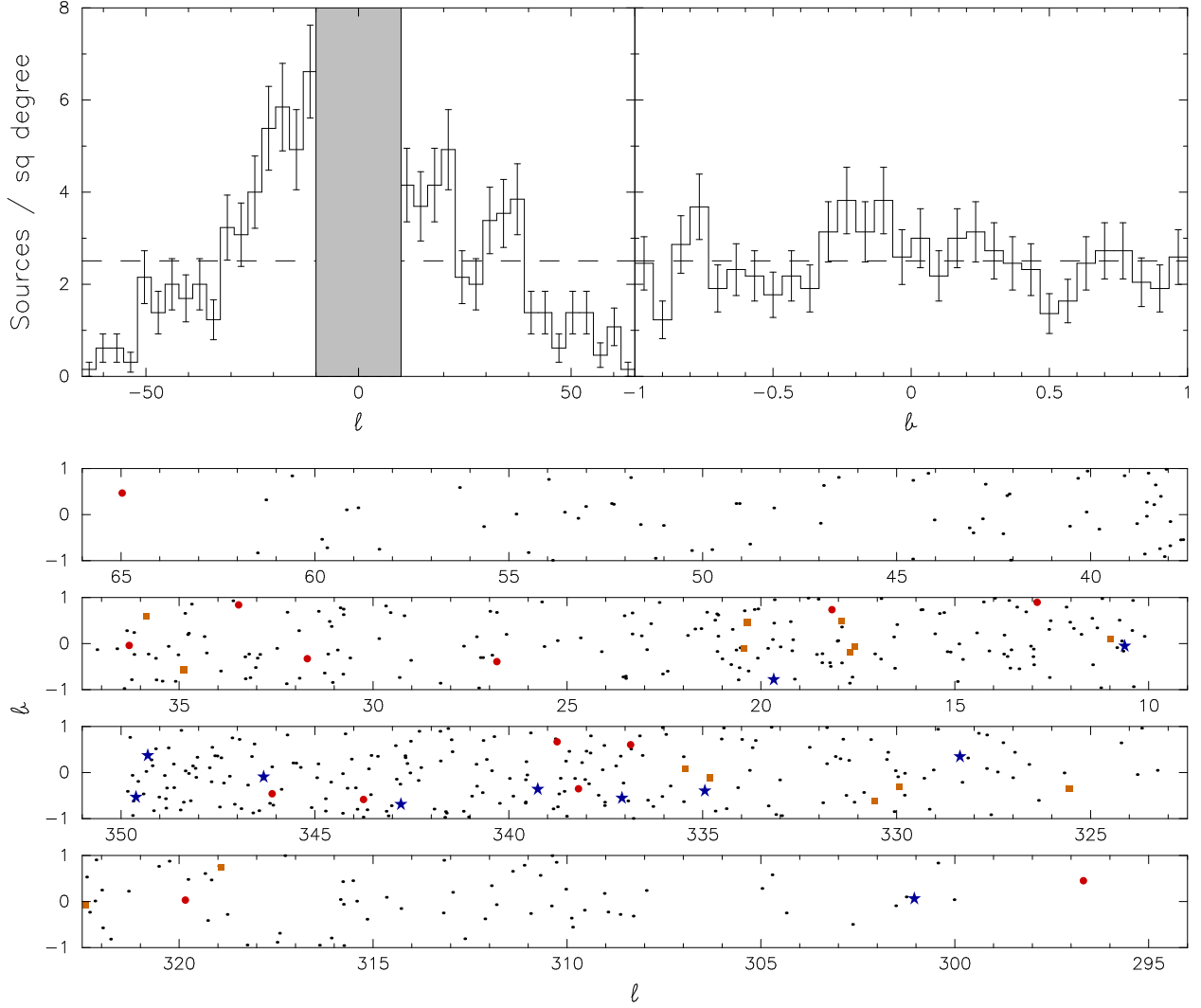


Fig. 10.— Top: Galactic longitude and latitude distribution of the 552 candidate variable stars. The dashed line shows the expected level for a uniform distribution. The error bars were calculated using Poisson statistics. Bottom: Spatial distribution of the candidate variable stars (sources where IRAC $8.0\mu\text{m}$ and MSX $8.28\mu\text{m}$ differ by more than a factor of 2). The dots represent sources in the whole sample of 552 sources. The stars show the location of the subset of sources where IRAC $8.0\mu\text{m}$ and MSX $8.28\mu\text{m}$ differ by more than a factor of 4, the circles show the sources where MSX $21.3\mu\text{m}$ and MIPS $24.0\mu\text{m}$ differ by more than a factor of two, and the squares show the sources where a mismatch between JHK_s and IRAC is present.

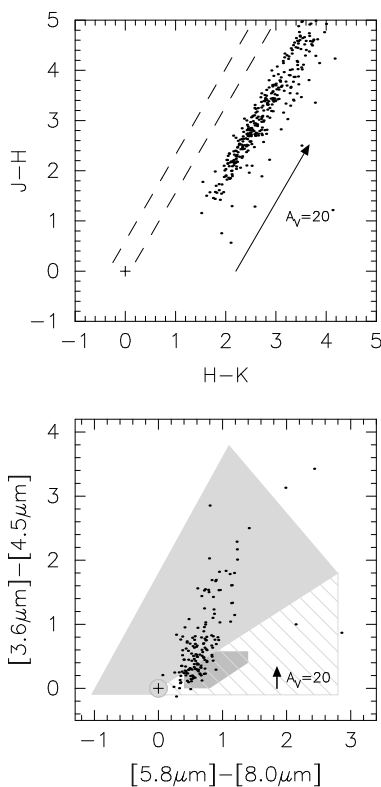


Fig. 11.— JHK (top) and IRAC (bottom) color-color plots of the variable star candidates. Only sources with all three 2MASS fluxes were used for the JHK color-color plot, and only sources with all four IRAC bands were used for the IRAC color-color plot. The cross marks the approximate location of un-reddened stars, and the reddening vectors show an extinction of $A_V=20$. The dashed lines in the top panel show where reddened stars would lie for a range of stellar temperatures. The filled and hashed areas in light gray in the bottom panel are adapted from Robitaille et al. (2006), and show where YSOs are expected to lie in IRAC color-color space.

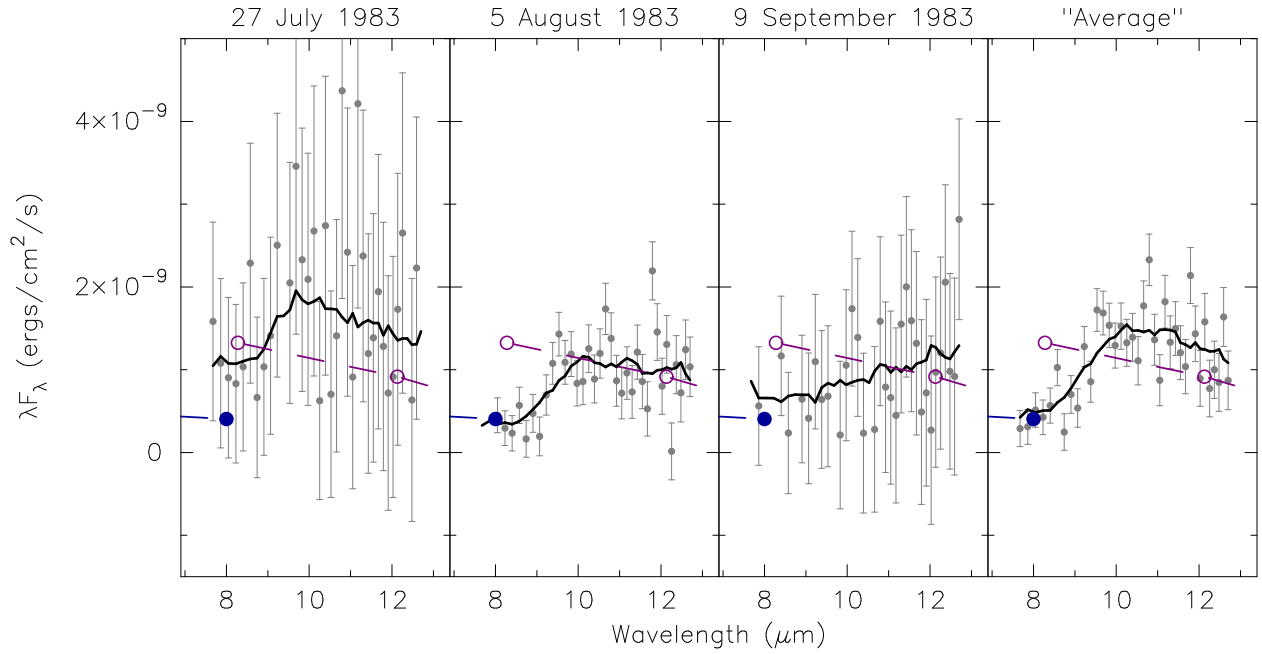


Fig. 12.— LRS Spectrum for G296.6843+00.4515 (IRAS 11557-6129) for three epochs, and the “Average” LRS spectrum (as defined in the IRAS Explanatory Supplement, Chapter IX.C.3). The points and error bars show the original calibrated spectra (with negative fluxes removed), and the solid lines show the data after smoothing the data by performing a ‘box optimal average’ at each point (the total width of the box was set to $1.5\mu\text{m}$). The larger open and closed circles, show the MSX and IRAC data respectively, and the dashed lines are equivalent to the solid lines in Figure 7.

Table 1. Sensitivity and saturation levels

Band	Sensitivity mJy	Saturation mJy
J	0.4	16000
H	0.6	16000
K _s	0.8	16000
IRAC 3.6 μ m	0.5	439
IRAC 4.5 μ m	0.5	450
IRAC 5.8 μ m	2.0	2930
IRAC 8.0 μ m	5.0	1590
MSX A	100→200	n/a ^a
MSX C	1100→3100	n/a ^a
MSX D	900→2000	n/a ^a
MSX E	2000→6000	n/a ^a
MIPS 24 μ m	2.6	1400

^aAccording to the Midcourse Space Experiment Point Source Catalog Version 1.2 Explanatory Guide, only four sources in the whole survey were saturated. The saturation limit is likely to be above 10⁶ mJy.

Note. — The above values are approximate, since they depend in some cases on factors such as confusion or background emission, and only apply to the surveys used in this paper. The 2MASS values are from the 2MASS All-Sky Data Release Explanatory Supplement (1.6), the IRAC values are from the GLIMPSE data products description, and the MSX sensitivity values are from the Midcourse Space Experiment Point Source Catalog Version 1.2 Explanatory Guide (Table 1). The MIPS 24.0 μ m values are from a private communication.

Table 2. The sample of 552 sources with apparent variability at $8\mu\text{m}$

MSX source name	GLIMPSE source name	Coordinates		2MASS			IRAC					MSX			MIPS	MSX Σvar^a	IRAS Var
		α (J2000) °	δ (J2000) °	F _J mJy	F _H mJy	F _{K_s} mJy	F _{3.6} mJy	F _{4.5} mJy	F _{5.8} mJy	F _{8.0} mJy	F _{8.28} mJy	F _{12.13} mJy	F _{14.65} mJy	F _{21.3} mJy	F ₂₄ mJy		
G010.1167+00.1543	SSTGLMC G010.1162+00.1539	271.85730	-20.11289	2.8	191.6	...	938.2	976.6	340.9	683.3	0	29
G010.3957-00.9373	SSTGLMC G010.3955-00.9365	273.01970	-20.39660	14.3	109.4	297.0	447.3	402.9	187.6	339.5	0	...
G010.4174+00.9357	SSTGLMC G010.4167+00.9355	271.28840	-19.46910	2.2	3.2	5.1	5.5	7.8	7.2	55.6	149.8	...	690.0	2139.9	2466.1	0	-1
G010.4355+00.2827	SSTGLMC G010.4351+00.2830	271.90300	-19.77190	0.5	13.9	100.6	647.1	537.6	215.7	564.3	1	...
G010.6179-00.0560	SSTGLMC G010.6180-00.0559	272.31180	-19.77690	6.1	309.8	...	1290.0	1149.0	291.3	378.0	1	13
G010.6616-00.1658	SSTGLMC G010.6622-00.1653	272.43640	-19.79180	...	5.7	147.1	1189.0	591.5	222.1	142.4	1	...
G010.7026+00.0569	SSTGLMC G010.7020+00.0568	272.25040	-19.64800	...	7.1	96.0	410.4	...	590.1	448.5	178.6	160.4	0	...
G010.7615+00.5088	SSTGLMC G010.7611+00.5091	271.86160	-19.37710	10.3	94.0	293.2	416.6	414.2	469.1	497.7	1216.3	1665.2	1156.4	...	895.5	1	...
G010.8254-00.0874	SSTGLMC G010.8249-00.0873	272.44760	-19.61050	...	4.2	45.7	281.4	379.0	454.1	356.3	185.0	159.4	0	-1
G010.9867+00.1010	SSTGLMC G010.9866+00.1011	272.35540	-19.37810	...	9.8	55.1	74.7	99.3	135.7	139.5	329.3	165.4	0	...
G011.2092+00.9780	SSTGLMC G011.2090+00.9777	271.65870	-18.75760	10.0	63.3	188.9	373.1	376.7	411.4	492.5	1682.1	2040.4	1300.1	1372.4	1231.8	0	93
G011.2352-00.9600	SSTGLMC G011.2353-00.9595	273.46920	-19.67080	...	4.9	14.2	108.6	306.4	627.6	1004.0	357.1	...	1411.4	1	-1
G011.3364+00.3392	SSTGLMC G011.3360+00.3395	272.31400	-18.95680	40.8	243.6	629.7	785.6	769.4	2352.1	2683.5	2078.2	...	1705.5	2	...
G011.4445-00.4598	SSTGLMC G011.4444-00.4590	273.11000	-19.24750	...	8.6	16.5	1122.0	1177.0	519.2	...	1084.2	...	1262.8	0	14
G011.4640+00.5500	SSTGLMC G011.4637+00.5500	272.18440	-18.74311	393.8	1784.0	3188.0	1063.0	771.2	1485.0	1823.7	1535.6	...	514.2	1	-1
G011.7438+00.2020	SSTGLMC G011.7431+00.2018	272.64890	-18.66651	46.8	175.5	348.6	344.6	273.0	263.5	222.2	430.4	205.8	0	...
G011.9397+00.3272	SSTGLMC G011.9392+00.3272	272.63290	-18.43450	150.7	608.0	1158.0	581.7	544.7	1328.0	1518.5	1049.1	...	506.8	0	...
G012.0350+00.4646	SSTGLMC G012.0344+00.4647	272.55460	-18.28470	13.4	100.7	268.1	595.4	422.4	218.9	129.5	1	...
G012.1287+00.7908	SSTGLMC G012.1282+00.7906	272.30170	-18.04500	18.6	129.6	332.6	345.3	265.9	269.4	243.6	500.1	345.9	0	...
G012.5376+00.4942	SSTGLMC G012.5370+00.4943	272.78230	-17.83020	2.0	67.5	416.8	689.1	541.0	1078.2	1445.6	1020.8	...	1219.9	0	...
G012.5638-00.7378	SSTGLMC G012.5632-00.7372	273.93340	-18.39750	38.2	248.4	535.0	...	395.6	407.6	506.9	1150.4	1909.8	1590.4	2118.8	2347.2	2	3
G012.5767+00.3086	SSTGLMC G012.5763+00.3089	272.97300	-17.88520	57.8	272.8	835.1	1439.0	560.2	...	1582.6	...	837.0	1	...
G012.8758+00.8954	SSTGLMC G012.8754+00.8952	272.58470	-17.34040	5.2	57.6	227.0	428.4	...	575.6	638.0	1303.6	1906.6	1507.7	2124.5	798.8	2	-1
G012.9387+00.9173	SSTGLMC G012.9385+00.9170	272.59640	-17.27480	47.2	194.8	336.6	375.8	311.0	148.1	166.6	0	...
G012.9661-00.4597	SSTGLMC G012.9661-00.4593	273.87780	-17.91130	...	1.9	46.3	365.4	...	750.2	712.0	198.7	413.7	0	...
G012.9745-00.1179	SSTGLMC G012.9738-00.1175	273.56659	-17.74070	...	1.2	60.3	1881.0	1206.0	623.7	...	827.9	...	368.5	0	...
G012.9874-00.2853	SSTGLMC G012.9875-00.2852	273.72750	-17.80930	...	1.7	40.3	355.1	...	819.3	546.9	244.9	164.6	0	...
G013.0456-00.0546	SSTGLMC G013.0451-00.0545	273.54390	-17.64800	12.6	321.6	...	1182.0	960.4	473.4	655.2	1	...
G013.1687+00.6897	SSTGLMC G013.1684+00.6898	272.92120	-17.18290	157.2	619.3	1192.0	1206.0	1203.0	637.4	918.3	0	...
G013.3467-00.5484	SSTGLMC G013.3463-00.5482	274.14991	-17.61880	...	6.8	44.8	434.6	...	908.6	942.5	432.7	485.4	0	...
G013.4040+00.7912	SSTGLMC G013.4038+00.7909	272.94650	-16.92780	425.8	434.3	497.7	456.0	946.0	243.6	0	...
G013.5503-00.1361	SSTGLMC G013.5502-00.1359	273.87150	-17.24340	19.1	290.7	...	645.7	582.4	185.4	233.8	0	...
G013.5764-00.5299	SSTGLMC G013.5762-00.5301	274.24740	-17.40780	...	2.5	36.4	1544.0	1468.0	539.9	...	1095.8	...	1172.9	1	...
G013.6088+00.9344	SSTGLMC G013.6087+00.9344	272.91821	-16.67940	3.7	23.7	89.3	270.2	252.4	291.7	324.0	667.5	772.0	740.7	...	502.7	0	...
G013.6518-00.2816	SSTGLMC G013.6519-00.2819	274.05620	-17.22350	19.9	334.1	...	1242.0	1196.0	462.4	...	822.3	...	463.7	1	...
G013.7291+00.1836	SSTGLMC G013.7291+00.1842	273.66681	-16.93370	432.7	...	1141.0	1357.0	550.0	850.4	989.5	1492.6	801.8	1	...
G013.7391-00.2278	SSTGLMC G013.7391-00.2277	274.05010	-17.12110	4.9	106.2	561.7	833.1	620.5	1203.5	1840.1	1426.5	...	823.0	0	...
G013.9733+00.9824	SSTGLMC G013.9732+00.9826	273.05690	-16.33680	2.8	50.8	201.5	345.0	295.0	306.3	267.4	618.5	533.0	0	...
G014.1190-00.1600	SSTGLMC G014.1189-00.1601	274.17660	-16.75470	397.0	...	1322.0	1248.0	582.1	...	1183.5	...	763.5	0	...
G014.2632+00.9057	SSTGLMC G014.2631+00.9058	273.27190	-16.11920	5.9	57.5	177.5	434.7	434.7	481.5	512.5	1210.6	1345.4	1277.1	...	802.2	0	11
G014.4391+00.2320	SSTGLMC G014.4397+00.2322	273.97579	-16.28660	224.6	250.2	293.8	304.1	552.5	292.7	0	...
G014.7987-00.3419	SSTGLMC G014.7994-00.3421	274.67990	-16.24250	19.9	258.2	820.2	1213.0	760.9	368.2	248.1	0	...
G014.8941-00.0095	SSTGLMC G014.8946-00.0096	274.42220	-16.00110	...	3.3	87.9	891.5	737.2	1671.2	2224.2	2305.9	...	981.0	0	11
G014.9333-00.8253	SSTGLMC G014.9336-00.8254	275.19000	-16.35220	...	3.2	33.9	360.6	...	724.2	730.6	1818.2	2722.3	2545.7	...	2179.1	2	...
G015.1163-00.1832	SSTGLMC G015.1165-00.1831	274.69070	-15.88770	...	7.9	77.7	952.4	1012.0	2442.4	3458.8	3498.1	...	3064.9	1	15
G015.1992-00.1757	SSTGLMC G015.1997-00.1756	274.72459	-15.81110	12.6	143.9	510.4	1333.0	1012.0	547.1	447.6	0	...
G015.2828+00.6737	SSTGLMC G015.2829+00.6736	273.98960	-15.33440	517.3	544.8	1169.4	1210.4	404.6	0	25
G015.3979+00.6502	SSTGLMC G015.3986+00.6499	274.06790	-15.24430	143.1	504.8	940.9	1086.0	1050.0	502.5	664.2	1	...
G015.5188+00.2132	SSTGLMC G015.5192+00.2138	274.52600	-15.34540	1.0	22.5	111.6	676.9	617.7	253.4	325.0	0	...

Table 2—Continued

MSX source name	GLIMPSE source name	Coordinates		2MASS			IRAC					MSX			MIPS	MSX Σ var ^a	IRAS Var
		α (J2000) °	δ (J2000) °	F _J mJy	F _H mJy	F _{K_s} mJy	F _{3.6} mJy	F _{4.5} mJy	F _{5.8} mJy	F _{8.0} mJy	F _{8.28} mJy	F _{12.13} mJy	F _{14.65} mJy	F _{21.3} mJy	F ₂₄ mJy		
G015.8394+00.7370	SSTGLMC G015.8396+00.7368	274.20600	-14.81470	24.7	97.8	191.8	211.6	158.1	157.2	147.7	299.5	118.6	0	...
G015.8797+00.7309	SSTGLMC G015.8802+00.7310	274.23140	-14.78220	29.4	127.6	276.9	...	445.5	388.2	390.5	999.0	1325.8	501.2	0	...
G016.4969+00.4134	SSTGLMC G016.4971+00.4130	274.82250	-14.38900	...	7.1	40.8	376.3	...	484.9	471.6	201.5	219.8	0	...
G016.5517-00.5357	SSTGLMC G016.5512-00.5352	275.71440	-14.78760	0.5	11.1	70.5	368.1	417.5	451.5	372.2	160.7	163.3	0	...
G016.5752+00.1448	SSTGLMC G016.5755+00.1445	275.10510	-14.44680	...	1.7	19.5	368.1	...	1273.0	1201.0	620.5	264.4	1	...
G016.9015+00.9756	SSTGLMC G016.9016+00.9753	274.50919	-13.76660	9.6	123.0	459.1	656.0	483.4	1184.5	...	1128.7	...	381.1	0	...
G016.9122-00.3372	SSTGLMC G016.9118-00.3371	275.70800	-14.37620	4.9	142.0	374.0	736.7	839.7	401.5	...	960.4	...	1834.7	1	0
G017.0637-00.2244	SSTGLMC G017.0642-00.2247	275.67861	-14.18950	2.6	75.8	438.9	1441.0	1042.0	341.0	208.7	1	...
G017.5692-00.0692	SSTGLMC G017.5696-00.0693	275.78170	-13.67020	16.4	150.2	497.4	420.6	...	593.8	641.6	1422.1	1724.7	1550.6	...	1875.7	1	...
G017.6490-00.7260	SSTGLMC G017.6494-00.7264	276.41800	-13.90700	217.9	...	950.2	927.7	423.5	256.7	1	...
G017.6991-00.1976	SSTGLMC G017.6993-00.1978	275.96109	-13.61570	4.0	55.7	239.2	287.2	375.8	518.3	560.2	1300.4	1678.1	1336.6	...	1359.6	0	...
G017.7153-00.8603	SSTGLMC G017.7157-00.8610	276.57210	-13.91100	564.9	400.7	179.1	106.0	0	...
G017.9183-00.4188	SSTGLMC G017.9185-00.4188	276.26770	-13.52540	74.8	469.4	1164.0	919.4	809.5	1902.2	2509.5	1814.2	1804.9	1245.4	3	99
G017.9203+00.3597	SSTGLMC G017.9203+00.3592	275.56180	-13.15890	11.2	85.6	245.2	562.7	486.5	151.5	248.8	1	...
G017.9268+00.4932	SSTGLMC G017.9269+00.4933	275.44380	-13.09040	40.0	192.8	406.9	254.8	226.3	242.4	247.6	674.2	184.1	0	...
G018.0174+00.0642	SSTGLMC G018.0179+00.0640	275.87650	-13.21180	20.3	133.6	384.4	697.6	740.8	1717.9	2238.2	1940.4	...	1525.5	1	7
G018.0346+00.0532	SSTGLMC G018.0353+00.0530	275.89480	-13.20170	4.6	95.2	414.9	1241.0	1134.0	507.1	...	771.2	...	459.1	0	...
G018.1666+00.7366	SSTGLMC G018.1665+00.7365	275.33920	-12.76430	220.9	704.5	1253.0	1095.0	1361.0	3290.1	3848.1	2463.1	2923.7	1243.2	1	99
G018.2086-00.4971	SSTGLMC G018.2090-00.4975	276.47820	-13.30530	...	7.1	64.1	322.9	415.0	584.9	544.1	238.4	467.9	1	...
G018.2271-00.4142	SSTGLMC G018.2278-00.4135	276.41180	-13.25020	0.8	12.3	63.8	1404.0	1219.0	564.3	673.6	1	...
G018.4233-00.2183	SSTGLMC G018.4233-00.2186	276.32790	-12.98520	14.1	205.9	276.2	403.1	446.9	1107.0	1607.1	1260.3	...	1177.6	1	...
G018.4287-00.4139	SSTGLMC G018.4288-00.4141	276.50810	-13.07180	20.1	201.7	679.1	1199.0	1231.0	2854.6	4324.6	3407.5	3682.5	...	0	...
G018.5213+00.9627	SSTGLMC G018.5214+00.9624	275.30580	-12.34500	1244.0	1455.0	742.0	966.9	513.1	0	-1
G018.5674-00.2364	SSTGLMC G018.5675-00.2366	276.41340	-12.86630	...	10.4	84.6	1477.0	1081.0	523.4	193.9	0	...
G018.7862+00.9864	SSTGLMC G018.7862+00.9868	275.41180	-12.10010	...	7.2	47.4	255.7	345.9	454.6	554.1	1421.3	1806.1	1587.2	...	1237.7	1	0
G019.1384-00.7703	SSTGLMC G019.1387-00.7704	277.17030	-12.60950	0.9	17.2	92.2	767.5	576.4	229.4	90.8	0	...
G019.1771+00.0849	SSTGLMC G019.1775+00.0850	276.41380	-12.17700	422.5	...	704.8	594.2	222.9	359.3	0	...
G019.2005-00.1562	SSTGLMC G019.2015-00.1564	276.64331	-12.26880	263.4	...	966.7	918.7	406.0	584.8	1	...
G019.2427+00.4746	SSTGLMC G019.2432+00.4748	276.09280	-11.93690	61.8	392.9	1119.0	1294.0	1291.0	3897.1	4734.4	3257.5	2958.0	2416.6	0	91
G019.5039-00.0708	SSTGLMC G019.5048-00.0709	276.71060	-11.96060	6.3	407.4	...	1011.0	893.1	270.2	312.3	1	...
G019.6527+00.9538	SSTGLMC G019.6529+00.9540	275.85650	-11.35029	41.9	178.3	383.6	388.8	369.4	688.3	506.9	0	31
G019.6672-00.7858	SSTGLMC G019.6675-00.7870	277.43560	-12.14820	17.1	1288.0	1223.0	247.5	505.1	0	...
G019.6687+00.4460	SSTGLMC G019.6691+00.4454	276.32210	-11.57370	649.1	643.7	310.4	405.9	1	...
G019.7004+00.0862	SSTGLMC G019.7009+00.0861	276.66210	-11.71350	24.9	2150.0	1500.0	639.6	361.4	1	...
G019.8247-00.1051	SSTGLMC G019.8258-00.1054	276.89420	-11.69260	1521.0	1201.0	464.2	354.1	1	...
G020.0776+00.7515	SSTGLMC G020.0779+00.7516	276.24140	-11.06950	745.6	784.1	323.6	323.8	0	...
G020.0895-00.3161	SSTGLMC G020.0897-00.3163	277.21050	-11.55630	56.3	325.9	712.4	...	408.7	408.1	388.4	908.0	1455.0	777.7	...	461.1	1	...
G020.1735+00.7416	SSTGLMC G020.1734+00.7416	276.29590	-10.98930	24.4	142.8	388.6	814.5	916.0	2109.6	2565.7	1751.7	...	642.9	1	6
G020.3270-00.5964	SSTGLMC G020.3271-00.5968	277.57640	-11.47580	8.3	80.7	270.4	1185.0	1028.0	357.1	388.1	1	...
G020.3407+00.4617	SSTGLMC G020.3405+00.4618	276.62760	-10.97200	...	27.4	119.8	110.7	182.8	275.6	369.2	1014.4	1383.4	1255.2	...	988.1	3	...
G020.4267+00.7107	SSTGLMC G020.4266+00.7107	276.44410	-10.77990	16.4	139.3	433.2	603.9	631.6	1569.3	1709.2	1357.3	...	1145.4	0	31
G020.4301-00.1046	SSTGLMC G020.4305-00.1044	277.18080	-11.15641	...	67.9	326.5	415.9	...	930.8	950.9	462.1	457.6	0	...
G020.5371-00.0914	SSTGLMC G020.5371-00.0918	277.21950	-11.05550	1.5	44.6	226.5	592.0	392.8	186.1	171.2	1	...
G020.5612-00.5220	SSTGLMC G020.5613-00.5222	277.61980	-11.23380	98.2	505.7	1078.0	1380.0	1040.0	537.5	586.0	568.2	2	...
G020.5859-00.7898	SSTGLMC G020.5861-00.7904	277.87350	-11.33580	21.1	156.6	445.8	851.4	806.8	341.6	430.2	380.6	...	391.0	1	...
G020.6422-00.1393	SSTGLMC G020.6425-00.1400	277.31240	-10.98470	4.1	286.1	...	1026.0	965.9	520.8	782.6	957.9	...	475.9	1	...
G020.7389+00.3096	SSTGLMC G020.7389+00.3094	276.95340	-10.69050	32.9	200.8	530.1	781.1	732.7	2260.1	2848.9	2215.4	2570.7	1744.7	2	99
G020.7748-00.4575	SSTGLMC G020.7749-00.4577	277.66230	-11.01470	4.9	58.8	196.2	417.2	...	477.3	455.1	206.7	415.3	183.2	1	...
G021.0014-00.3329	SSTGLMC G021.0015-00.3334	277.65670	-10.75610	319.8	1034.0	1723.0	963.6	595.2	1003.4	839.2	578.4	...	193.4	1	...

Table 2—Continued

MSX source name	GLIMPSE source name	Coordinates		2MASS			IRAC					MSX			MIPS	MSX \sum var ^a	IRAS Var
		α (J2000) °	δ (J2000) °	F _J mJy	F _H mJy	F _{K_s} mJy	F _{3.6} mJy	F _{4.5} mJy	F _{5.8} mJy	F _{8.0} mJy	F _{8.28} mJy	F _{12.13} mJy	F _{14.65} mJy	F _{21.3} mJy	F ₂₄ mJy	mJy	%
G021.1053+00.6189	SSTGLMC G021.1053+00.6186	276.84820	-10.22220	245.1	636.1	1049.0	1362.0	1204.0	585.9	585.6	469.2	...	659.9	1	...
G021.1069+00.1587	SSTGLMC G021.1067+00.1590	277.26320	-10.43470	241.6	264.8	299.3	255.2	91.3	135.1	0	...
G021.1332-00.1710	SSTGLMC G021.1338-00.1712	277.57280	-10.56430	...	35.3	161.4	1207.0	1240.0	469.7	788.2	765.1	...	717.0	2	...
G021.1393+00.6447	SSTGLMC G021.1394+00.6445	276.84120	-10.18010	28.5	171.2	465.9	1010.0	1161.0	643.7	768.9	618.5	...	506.8	1	...
G021.1903+00.5095	SSTGLMC G021.1902+00.5091	276.98690	-10.19780	18.6	120.6	294.5	658.1	562.5	314.9	195.2	0	...
G021.3966+00.6815	SSTGLMC G021.3965+00.6815	276.92960	-9.93530	48.6	184.3	306.4	349.4	280.5	240.9	168.6	75.8	22.3	0	...
G021.5432+00.3223	SSTGLMC G021.5431+00.3221	277.32170	-9.97230	0.9	15.4	100.6	1321.0	1123.0	579.6	316.4	1	...
G021.7022+00.3175	SSTGLMC G021.7025+00.3175	277.40090	-9.83370	1.1	23.3	136.1	1134.0	1195.0	613.4	...	948.8	...	621.0	0	...
G021.8923+00.1770	SSTGLMC G021.8925+00.1768	277.61660	-9.73030	...	4.2	53.1	406.7	...	1082.0	1071.0	462.9	...	1051.3	...	611.4	1	...
G022.4131-00.6005	SSTGLMC G022.4123-00.6002	278.56030	-9.62760	0.8	7.3	45.1	343.7	...	549.1	540.4	245.9	599.7	0	...
G022.5394-00.6609	SSTGLMC G022.5395-00.6609	278.67370	-9.54330	7.4	206.8	...	853.9	934.9	433.5	294.6	0	...
G022.6245+00.8923	SSTGLMC G022.6245+00.8919	277.31830	-8.75001	28.1	117.5	232.7	263.6	184.0	174.2	133.6	251.3	92.9	0	...
G022.8406+00.4341	SSTGLMC G022.8405+00.4339	278.83050	-8.77080	...	35.8	186.7	873.7	756.9	374.5	974.1	0	...
G022.9473-00.1323	SSTGLMC G022.9473-00.1325	278.38880	-8.93770	...	12.4	139.3	337.5	435.5	566.0	431.5	971.7	...	1602.5	...	711.6	0	...
G023.0816+00.1692	SSTGLMC G023.0813+00.1692	278.18080	-8.67950	...	2.2	55.1	1787.0	1304.0	675.7	1185.8	821.0	...	453.6	1	...
G023.3191+00.2098	SSTGLMC G023.3188+00.2100	278.25520	-8.45000	10.6	305.2	...	908.5	849.2	359.2	398.2	1	...
G023.3210+00.6626	SSTGLMC G023.3206+00.6624	277.85020	-8.23910	28.0	155.8	363.0	676.8	631.7	343.0	227.9	0	...
G023.4895-00.7548	SSTGLMC G023.4895-00.7548	279.20060	-8.74300	252.9	223.4	275.7	214.0	515.3	228.4	1	...
G023.4914-00.7086	SSTGLMC G023.4913-00.7084	279.16000	-8.72001	15.5	99.3	368.1	751.5	278.8	614.3	0	...
G023.5247+00.6039	SSTGLMC G023.5247+00.6039	277.99790	-8.08560	1250.0	1152.0	2855.3	3406.3	2774.7	2494.9	1844.3	0	-1
G023.5601-00.7245	SSTGLMC G023.5598-00.7245	279.20620	-8.66630	7.6	86.6	317.1	1328.0	1239.0	559.5	580.1	1	...
G024.1139-00.1742	SSTGLMC G024.1136-00.1739	278.96961	-7.92150	165.5	...	1009.0	1021.0	474.5	...	1205.1	1937.1	...	1	...
G024.6558+00.1228	SSTGLMC G024.6557+00.1223	278.95490	-7.30370	...	6.0	78.6	1443.0	1220.0	564.4	935.8	1056.0	...	1099.0	2	...
G025.2515+00.0620	SSTGLMC G025.2516+00.0619	279.28520	-6.80260	30.8	323.6	...	1048.0	1152.0	414.2	829.1	813.4	...	1407.3	1	-1
G025.5928-00.0641	SSTGLMC G025.5927-00.0647	279.55590	-6.55740	...	2.1	31.1	1040.0	973.0	288.2	940.8	1	...
G025.6520+00.9055	SSTGLMC G025.6520+00.9059	278.71680	-6.05910	39.2	232.6	572.2	676.0	584.1	1467.2	1756.2	1424.2	...	1041.0	1	49
G026.5719+00.2006	SSTGLMC G026.5714+00.2006	279.77090	-5.56590	...	2.9	35.8	369.7	...	930.4	733.8	358.0	191.5	1	...
G026.8076-00.3922	SSTGLMC G026.8077-00.3920	280.40890	-5.62799	105.5	583.3	1226.0	925.1	866.3	2218.1	2532.5	1701.4	2397.0	794.6	1	...
G026.8173+00.6740	SSTGLMC G026.8170+00.6744	279.46140	-5.13070	16.2	116.8	295.1	326.5	231.4	253.9	225.9	467.7	511.1	1	...
G026.9347-00.2531	SSTGLMC G026.9348-00.2532	280.34309	-5.45130	1338.0	1269.0	567.4	936.0	755.4	0	...
G026.9882+00.6996	SSTGLMC G026.9879+00.6999	279.51730	-4.96710	4.7	47.4	239.0	1396.0	1538.0	3927.4	4922.5	4071.0	3828.4	2154.5	0	82
G027.1740-00.3042	SSTGLMC G027.1745-00.3039	280.49870	-5.26180	1044.0	2493.0	3551.0	1649.0	1166.0	397.3	500.0	0	-1
G027.2371-00.3023	SSTGLMC G027.2369-00.3020	280.52600	-5.20489	178.5	832.3	1589.0	780.8	755.7	1863.3	2411.8	1614.7	...	718.1	3	99
G027.2775-00.9632	SSTGLMC G027.2775-00.9630	281.13500	-5.47090	15.7	97.8	271.4	389.7	...	566.5	603.3	1497.0	1825.3	1231.5	...	1096.7	1	...
G027.3360+00.1473	SSTGLMC G027.3363+00.1474	280.17000	-4.91110	...	11.1	95.5	409.6	...	1298.0	1452.0	3694.4	5821.1	5942.8	5349.0	3501.7	0	...
G027.6672-00.0548	SSTGLMC G027.6673-00.0547	280.50260	-4.70921	27.3	142.2	431.8	976.8	1169.0	3069.1	4642.6	5582.3	6000.8	...	0	95
G028.2726-00.8580	SSTGLMC G028.2721-00.8584	281.49680	-4.53760	51.0	184.1	313.9	211.4	166.7	162.0	173.1	385.8	190.2	0	...
G029.0313-00.3624	SSTGLMC G029.0310-00.3625	281.40190	-3.63640	1.4	18.8	105.7	991.6	808.9	369.6	142.7	1	...
G029.2002+00.6025	SSTGLMC G029.2001+00.6026	280.61930	-3.04530	71.3	359.0	779.0	967.4	790.3	423.0	336.1	1	...
G029.3232-00.7340	SSTGLMC G029.3230-00.7341	281.86660	-3.54620	...	6.7	114.1	1334.0	1149.0	498.3	921.2	1	...
G029.5562+00.6706	SSTGLMC G029.5561+00.6706	280.72159	-2.69750	39.6	211.4	618.8	877.2	1009.0	2763.1	3330.1	2510.1	2385.7	1286.2	1	99
G029.6751+00.8147	SSTGLMC G029.6749+00.8146	280.64770	-2.52590	257.1	749.4	1160.0	...	386.9	388.9	433.3	1142.1	976.9	1	39
G029.8514+00.1090	SSTGLMC G029.8509+00.1092	281.35680	-2.69160	2.0	46.5	266.6	1370.0	1318.0	2658.3	3619.6	2935.7	2804.4	1691.3	3	99
G030.5988-00.3133	SSTGLMC G030.5983-00.3133	282.07430	-2.21920	...	4.0	31.2	994.0	695.9	354.6	156.4	0	...
G030.7669+00.7478	SSTGLMC G030.7669+00.7477	281.20630	-1.58530	468.7	502.9	1058.6	1339.5	1114.7	...	483.6	0	11
G030.7701+00.6269	SSTGLMC G030.7700+00.6266	281.31540	-1.63770	...	7.3	45.2	371.6	439.9	491.8	475.4	203.1	476.7	1	...
G030.7801-00.6647	SSTGLMC G030.7799-00.6649	282.47000	-2.21820	0.4	13.3	90.1	411.4	...	739.3	767.9	336.7	943.5	1	...
G030.8483+00.7765	SSTGLMC G030.8482+00.7763	281.21790	-1.49990	169.9	796.3	1577.0	694.6	503.0	1110.7	713.5	0	...
G030.9196-00.1415	SSTGLMC G030.9194-00.1416	282.06770	-1.85540	2.8	83.9	429.3	1211.0	814.1	374.5	286.3	1	...

Table 2—Continued

MSX source name	GLIMPSE source name	Coordinates		2MASS			IRAC				MSX			MIPS	MSX Σ var ^a	IRAS Var	
		α (J2000) °	δ (J2000) °	F _J mJy	F _H mJy	F _{K_s} mJy	F _{3.6} mJy	F _{4.5} mJy	F _{5.8} mJy	F _{8.0} mJy	F _{8.28} mJy	F _{12.13} mJy	F _{14.65} mJy	F _{21.3} mJy	F ₂₄ mJy		%
G031.0499−00.8426	SSTGLMC G031.0497−00.8425	282.75150	−2.05910	25.6	166.7	405.8	335.8	323.9	357.5	385.3	1108.7	1401.4	1122.4	...	452.9	0	91
G031.0765+00.3711	SSTGLMC G031.0763+00.3715	281.68290	−1.48190	...	1.2	21.0	433.2	...	829.9	732.1	292.8	1030.5	0	...
G031.1282+00.4787	SSTGLMC G031.1281+00.4788	281.61080	−1.38680	...	36.1	136.8	829.1	583.9	293.5	134.5	1	...
G031.1661−00.2286	SSTGLMC G031.1660−00.2285	282.25780	−1.67580	0.5	22.5	151.3	560.1	484.2	1062.4	1502.6	1187.2	...	714.4	1	...
G031.2598−00.6415	SSTGLMC G031.2597−00.6414	282.66820	−1.78060	...	1.5	13.1	240.4	...	706.0	777.3	299.3	...	673.1	...	829.9	1	...
G031.4121+00.6991	SSTGLMC G031.4120+00.6984	281.54410	−1.03360	5.9	58.2	177.3	367.4	303.4	307.6	249.7	457.2	255.3	0	...
G031.6975−00.3260	SSTGLMC G031.6973−00.3259	282.58689	−1.24730	...	2.0	15.8	228.6	402.7	697.9	845.4	2628.4	3750.1	3129.3	2846.0	1350.7	0	98
G031.9060−00.7515	SSTGLMC G031.9065−00.7514	283.06080	−1.25570	47.8	151.9	277.2	268.2	204.8	183.8	161.7	378.1	223.9	0	...
G031.9176+00.2806	SSTGLMC G031.9174+00.2805	282.14730	−0.77470	21.9	161.0	443.3	1163.0	1093.0	482.7	777.7	0	...
G032.2159+00.6784	SSTGLMC G032.2159+00.6782	281.92930	−0.32780	660.6	589.3	1212.3	1562.2	609.0	2	...
G032.2381−00.8718	SSTGLMC G032.2384−00.8716	283.31920	−1.01500	76.7	253.0	432.4	281.3	201.6	226.9	234.8	534.3	174.9	0	...
G032.4862−00.1047	SSTGLMC G032.4862−00.1047	282.74960	−0.44440	10.5	94.7	275.1	...	411.3	410.5	345.9	770.5	314.2	0	...
G032.9204−00.2348	SSTGLMC G032.9205−00.2350	283.06339	−0.11730	...	15.8	135.4	1059.0	1096.0	581.8	956.6	1066.1	1154.1	2178.5	2	...
G032.9867−00.3147	SSTGLMC G032.9868−00.3152	283.16470	−0.09470	306.8	...	981.4	1127.0	333.6	506.5	527.1	...	1258.4	0	...
G033.0343−00.5218	SSTGLMC G033.0344−00.5221	283.37070	−0.14670	5.4	52.1	181.4	248.4	253.8	282.6	293.2	707.7	972.0	694.8	703.3	379.3	1	...
G033.1729−00.7392	SSTGLMC G033.1732−00.7394	283.62740	−0.12250	27.5	160.8	421.1	395.0	335.7	392.0	423.7	1089.0	1316.6	990.3	942.6	473.1	3	0
G033.2071−00.2298	SSTGLMC G033.2072−00.2299	283.18960	0.14020	...	7.0	46.6	212.7	271.7	356.6	393.0	935.7	1166.3	1051.9	...	409.5	1	...
G033.2942−00.7650	SSTGLMC G033.2944−00.7651	283.70570	−0.02640	231.7	659.3	977.1	...	449.4	477.9	524.0	1208.8	1290.4	995.6	915.1	490.2	1	...
G033.3071−00.2892	SSTGLMC G033.3070−00.2894	283.28810	0.20200	...	2.8	28.8	271.5	...	862.8	960.1	523.6	597.3	558.1	...	466.1	1	...
G033.4658+00.8407	SSTGLMC G033.4657+00.8406	282.35470	0.85860	141.0	649.1	1319.0	589.4	564.1	1397.8	1497.5	1133.6	1185.2	493.9	0	99
G033.6126+00.9263	SSTGLMC G033.6128+00.9264	282.34540	1.02819	...	3.0	35.7	131.0	260.4	439.3	541.0	1314.3	2049.3	1730.7	...	1238.7	1	0
G033.9332−00.5954	SSTGLMC G033.9330−00.5958	283.84610	0.61960	3.3	25.2	78.0	172.5	163.8	184.0	204.7	386.9	169.8	1	...
G034.2960−00.2027	SSTGLMC G034.2958−00.2027	283.66220	1.12150	...	7.0	64.9	350.7	407.6	511.4	489.2	261.2	493.2	0	...
G034.3567+00.1504	SSTGLMC G034.3566+00.1503	283.37550	1.33670	...	4.7	81.3	2010.0	1389.0	630.0	436.6	1	...
G034.6815+00.8550	SSTGLMC G034.6816+00.8551	282.89620	1.94700	1.7	19.0	108.3	374.5	898.6	1776.5	1861.2	...	2002.1	0	...
G034.7591+00.2254	SSTGLMC G034.7590+00.2254	283.49230	1.72900	5.5	40.0	95.3	185.0	225.8	551.6	...	972.9	...	412.6	0	...
G034.7835+00.1943	SSTGLMC G034.7836+00.1942	283.53110	1.73650	...	9.8	109.2	1094.0	827.7	409.8	109.6	0	...
G034.8556+00.6575	SSTGLMC G034.8558+00.6574	283.15150	2.01191	16.3	178.6	596.9	908.1	654.7	1449.3	1764.5	1343.4	...	564.4	0	78
G034.8787−00.5619	SSTGLMC G034.8785−00.5622	284.24780	1.47620	2.0	37.0	229.5	344.3	...	987.0	1405.0	3651.1	4806.0	4019.2	3579.4	1824.2	0	99
G035.0281−00.2440	SSTGLMC G035.0280−00.2442	284.03310	1.75420	0.9	22.1	109.3	356.7	448.9	556.6	466.0	188.0	159.5	0	...
G035.1031−00.8195	SSTGLMC G035.1031−00.8197	284.57960	1.55820	...	1.6	10.5	64.5	118.5	228.4	378.4	870.8	1774.2	2277.2	2232.5	1139.3	2	...
G035.2797−00.0600	SSTGLMC G035.2792−00.0602	283.98410	2.06211	0.2	11.2	89.8	270.6	291.9	333.6	349.1	671.1	1221.7	884.2	...	684.0	1	...
G035.4394−00.8150	SSTGLMC G035.4396−00.8148	284.72920	1.85950	...	9.4	73.2	194.2	236.1	318.3	336.5	791.1	1002.4	996.0	...	407.3	0	...
G035.5933−00.7863	SSTGLMC G035.5932−00.7865	284.77400	2.00940	83.3	606.9	1398.0	1517.0	1027.0	552.0	379.8	1	...
G035.6085−00.3200	SSTGLMC G035.6082−00.3200	284.36570	2.23590	1.6	37.2	178.1	693.6	595.4	277.0	338.4	0	...
G035.7984−00.2285	SSTGLMC G035.7985−00.2285	284.37110	2.44660	3.4	67.4	298.6	376.5	393.2	455.4	431.1	957.6	1254.6	1055.1	...	453.0	0	−1
G035.8416+00.5887	SSTGLMC G035.8411+00.5890	283.66280	2.85800	...	51.1	198.2	79.6	173.4	327.9	519.9	1215.3	1430.2	1698.2	...	1532.7	2	97
G036.1665−00.2367	SSTGLMC G036.1663−00.2371	284.54660	2.77040	871.4	843.3	315.1	1078.4	1	...
G036.1698+00.2394	SSTGLMC G036.1695+00.2392	284.12390	2.99070	10.1	136.1	357.0	733.5	970.7	2383.7	3332.0	3734.8	2658.4	2018.6	1	99
G036.2301−00.7849	SSTGLMC G036.2299−00.7851	285.06390	2.57640	0.6	13.8	83.0	1116.0	902.0	447.1	240.2	0	...
G036.2908−00.0402	SSTGLMC G036.2906−00.0404	284.42850	2.97070	319.6	...	735.4	778.4	1998.2	3461.5	3378.2	3400.7	1582.3	0	96
G036.3534+00.2808	SSTGLMC G036.3535+00.2804	284.17100	3.17300	12.3	138.4	423.8	554.5	392.6	146.9	122.7	0	...
G036.4198−00.9770	SSTGLMC G036.4199−00.9772	285.32180	2.65730	8.4	78.9	244.1	829.2	792.5	407.8	0	...
G036.6056−00.1134	SSTGLMC G036.6054−00.1137	284.63771	3.21730	35.9	1427.0	1331.0	484.2	1805.4	0	...
G037.1208−00.1331	SSTGLMC G037.1205−00.1333	284.89100	3.66650	...	7.3	65.2	1193.0	1291.0	549.3	...	1006.9	...	1873.2	0	96
G037.6194−00.5445	SSTGLMC G037.6194−00.5444	285.48630	3.92180	1.1	32.9	187.4	1212.0	1205.0	666.5	...	784.5	...	1060.8	1	...
G037.6804−00.5460	SSTGLMC G037.6807−00.5463	285.51560	3.97530	...	1.7	13.3	39.9	74.5	127.9	158.3	309.6	207.7	0	...
G037.9492−00.1513	SSTGLMC G037.9492−00.1515	285.28710	4.39490	...	3.4	39.7	151.5	184.3	260.6	227.3	387.3	313.3	0	...
G037.9562−00.8742	SSTGLMC G037.9567−00.8744	285.75640	4.16180	0.7	16.5	94.0	329.7	378.6	399.4	371.2	178.7	323.5	0	...

Table 2—Continued

MSX source name	GLIMPSE source name	Coordinates		2MASS			IRAC					MSX			MIPS	MSX Σ var ^a	IRAS Var
		α (J2000) °	δ (J2000) °	F _J mJy	F _H mJy	F _{K_s} mJy	F _{3.6} mJy	F _{4.5} mJy	F _{5.8} mJy	F _{8.0} mJy	F _{8.28} mJy	F _{12.13} mJy	F _{14.65} mJy	F _{21.3} mJy	F ₂₄ mJy		
G038.0548+00.9853	SSTGLMC G038.0553+00.9854	284.32090	5.00830	...	2.8	19.8	276.8	342.2	419.3	350.6	160.9	0	...
G038.0962-00.9123	SSTGLMC G038.0966-00.9120	286.03290	4.17710	36.3	156.9	313.6	269.0	224.7	222.9	189.7	364.5	124.6	0	...
G038.1970+00.3969	SSTGLMC G038.1974+00.3971	284.91150	4.86610	48.2	281.8	537.0	...	403.2	393.8	291.1	129.5	112.3	0	...
G038.2234-00.7379	SSTGLMC G038.2235-00.7379	285.93599	4.37010	5.8	50.3	136.6	173.0	145.2	150.6	129.7	299.5	212.6	0	...
G038.3293+00.6455	SSTGLMC G038.3293+00.6463	284.75020	5.09730	20.1	149.9	333.5	...	404.5	389.8	283.8	140.7	83.4	0	...
G038.3704+00.2142	SSTGLMC G038.3707+00.2138	285.15420	4.93670	11.2	200.2	346.8	509.6	438.3	203.6	132.2	0	...
G038.5170+00.8999	SSTGLMC G038.5173+00.8998	284.60910	5.38040	13.7	124.8	323.8	362.6	229.8	229.1	201.8	491.6	194.9	0	...
G038.5595-00.0372	SSTGLMC G038.5600-00.0376	285.46550	4.98980	...	4.7	85.3	1155.0	891.6	440.0	383.7	1	...
G038.5613+00.2669	SSTGLMC G038.5617+00.2666	285.19480	5.13060	9.7	104.7	298.6	421.3	406.7	386.1	309.2	143.8	124.2	1	...
G038.6109-00.8574	SSTGLMC G038.6109-00.8571	286.22070	4.65960	1255.0	1176.0	667.0	712.0	0	83
G038.8130-00.1945	SSTGLMC G038.8131-00.1945	285.72240	5.14310	7.4	130.7	547.9	1503.0	1010.0	565.9	976.1	632.5	...	364.3	0	...
G039.1339+00.8431	SSTGLMC G039.1341+00.8430	284.94300	5.90330	2.8	33.9	164.7	1310.0	976.4	521.7	232.7	1	...
G039.7829-00.3167	SSTGLMC G039.7829-00.3178	286.27840	5.94900	1.0	23.6	110.8	372.7	...	448.8	320.2	161.7	53.7	0	...
G040.0875+00.9435	SSTGLMC G040.0878+00.9433	285.29160	6.79720	4.3	38.8	167.8	1509.0	1186.0	603.4	0	...
G040.1137+00.0558	SSTGLMC G040.1140+00.0551	286.09810	6.41390	108.7	629.7	1494.0	1368.0	1378.0	4180.6	5075.9	3606.1	3683.7	...	0	87
G040.3288+00.7876	SSTGLMC G040.3282+00.7872	285.54240	6.94040	95.8	366.0	700.7	589.1	578.7	1363.9	1562.9	1079.5	...	415.7	0	9
G040.5395-00.2524	SSTGLMC G040.5397-00.2529	286.57050	6.65060	554.8	622.5	1499.7	1744.7	1565.9	1918.4	1454.9	1	99
G042.0632-00.9870	SSTGLMC G042.0633-00.9871	287.93540	7.66400	0.6	5.5	17.5	200.8	267.6	356.3	463.5	1056.8	...	1060.1	2	94
G042.0972+00.4460	SSTGLMC G042.0975+00.4458	286.66710	8.35511	...	25.0	141.1	1555.0	1555.0	773.6	915.5	1	...
G042.1612+00.4103	SSTGLMC G042.1613+00.4098	286.72890	8.39550	173.8	694.2	1312.0	1362.0	1153.0	612.2	592.3	0	0
G042.2614-00.4152	SSTGLMC G042.2616-00.4160	287.51590	8.10390	...	8.2	58.8	247.0	260.6	279.7	249.3	110.9	205.0	1	...
G042.7177+00.6590	SSTGLMC G042.7176+00.6589	286.76440	9.00390	32.9	221.2	593.6	1550.0	1068.0	583.1	146.1	1	...
G042.7888-00.0916	SSTGLMC G042.7888-00.0917	287.47189	8.72120	193.9	1325.0	3078.0	2245.0	1472.0	795.7	900.5	287.1	0	...
G043.0271-00.3952	SSTGLMC G043.0274-00.3958	287.85570	8.79230	22.8	281.5	988.8	1274.0	1411.0	3142.1	3747.4	3012.0	2624.0	1489.7	1	...
G043.1266-00.2870	SSTGLMC G043.1268-00.2875	287.80510	8.93050	...	1.1	14.6	1217.0	1052.0	468.6	171.6	0	...
G044.0317-00.1159	SSTGLMC G044.0310-00.1163	288.07590	9.81200	1.0	20.6	96.0	246.2	340.7	368.6	264.8	135.9	33.0	0	...
G044.1921+00.8954	SSTGLMC G044.1922+00.8948	287.24000	10.42150	36.2	128.2	215.5	250.7	175.4	172.7	147.5	338.0	114.1	0	...
G044.5819+00.7455	SSTGLMC G044.5818+00.7451	287.55820	10.69820	2.0	30.1	144.5	1306.0	1504.0	692.1	932.6	872.5	920.7	953.7	1	...
G044.5885-00.9635	SSTGLMC G044.5883-00.9637	289.10030	9.91140	33.7	163.5	363.7	378.9	317.3	322.3	317.5	651.3	699.9	478.5	...	232.6	0	37
G046.4992+00.8092	SSTGLMC G046.4994+00.8092	288.40600	12.42720	1.5	22.8	188.7	986.0	2157.9	5210.9	6948.6	5955.9	...	1	98
G046.8864+00.6335	SSTGLMC G046.8866+00.6334	288.74960	12.68860	38.8	182.8	358.0	...	326.0	320.5	303.1	748.1	338.4	0	...
G046.9647-00.1868	SSTGLMC G046.9647-00.1864	289.53050	12.37530	12.4	128.1	392.2	867.3	918.8	434.6	702.1	1	52
G048.1694+00.1426	SSTGLMC G048.1691+00.1424	289.81040	13.59409	19.2	146.4	361.0	...	423.9	422.4	358.2	170.3	210.1	1	...
G048.7860-00.6395	SSTGLMC G048.7858-00.6403	290.81930	13.77030	8.9	120.4	454.1	1376.0	1290.0	593.9	982.3	936.7	1	23
G049.0589+00.2417	SSTGLMC G049.0593+00.2410	290.15030	14.42610	25.6	197.1	493.3	723.7	526.0	255.7	197.4	1	...
G049.1440+00.2415	SSTGLMC G049.1444+00.2416	290.19170	14.50120	6.8	81.7	286.2	1609.0	1583.0	694.2	653.1	0	3
G049.7644-00.7594	SSTGLMC G049.7641-00.7594	291.40590	14.57530	15.7	122.3	354.4	696.0	799.0	1913.4	1993.6	1449.2	1778.0	1377.3	1	99
G050.2859-00.7815	SSTGLMC G050.2857-00.7819	291.68230	15.02360	24.0	166.7	436.9	1197.0	1317.0	698.2	1048.9	827.5	1	97
G051.0147-00.2345	SSTGLMC G051.0144-00.2347	291.54271	15.92480	7.4	87.6	331.4	980.1	1170.0	484.4	762.6	1	...
G051.2204-00.9497	SSTGLMC G051.2205-00.9499	292.29810	15.76450	1.8	45.4	319.4	817.0	965.4	2398.7	4429.4	4177.6	4006.7	4181.0	0	98
G051.6086-00.2148	SSTGLMC G051.6082-00.2150	291.81900	16.45650	6.7	47.7	139.9	886.1	931.6	2119.9	2505.6	2080.7	...	1438.7	1	20
G051.8575+00.8056	SSTGLMC G051.8575+00.8056	291.00420	17.16010	4.2	68.1	325.6	1034.0	798.6	402.3	123.4	0	...
G052.3016+00.2227	SSTGLMC G052.3010+00.2227	291.76200	17.27431	6.8	67.9	233.3	651.1	824.6	1741.2	1953.8	1949.8	...	1636.0	1	95
G052.3552+00.2414	SSTGLMC G052.3548+00.2411	291.77150	17.33040	5.4	63.6	276.9	1284.0	1046.0	550.1	151.9	0	...
G053.0195+00.1766	SSTGLMC G053.0190+00.1764	292.16390	17.88320	8.6	29.6	70.7	135.1	185.2	235.9	280.6	542.2	500.8	0	68
G053.2176-00.0808	SSTGLMC G053.2176-00.0809	292.50110	17.93380	5.7	23.7	75.6	427.5	...	788.3	1090.0	343.9	3270.1	1	7
G053.5664+00.0539	SSTGLMC G053.5657+00.0535	292.55280	18.30440	...	2.7	40.4	1440.0	1313.0	587.3	594.2	0	...
G053.8738-00.9919	SSTGLMC G053.8742-00.9919	293.67310	18.06880	337.4	794.9	1163.0	687.3	572.9	1164.5	...	926.2	...	343.7	1	47
G053.9792+00.7638	SSTGLMC G053.9794+00.7633	292.10370	19.00680	93.3	241.6	327.7	244.7	176.5	150.5	113.9	213.6	49.9	1	...

Table 2—Continued

MSX source name	GLIMPSE source name	Coordinates		2MASS			IRAC					MSX			MIPS	MSX \sum var ^a	IRAS Var
		α (J2000) °	δ (J2000) °	F _J mJy	F _H mJy	F _{K_s} mJy	F _{3.6} mJy	F _{4.5} mJy	F _{5.8} mJy	F _{8.0} mJy	F _{8.28} mJy	F _{12.13} mJy	F _{14.65} mJy	F _{21.3} mJy	F ₂₄ mJy	mJy	
G054.4981−00.8238	SSTGLMC G054.4985−00.8238	293.83790	18.69610	439.5	378.0	896.6	1051.2	278.1	0	...
G054.8121+00.0139	SSTGLMC G054.8123+00.0138	293.22380	19.37690	13.3	103.4	261.0	1034.0	944.6	2439.4	2824.9	2280.0	1669.2	1167.6	2	99
G055.6494−00.2592	SSTGLMC G055.6500−00.2593	293.90880	19.97660	1.2	55.7	148.1	292.8	318.3	133.9	435.0	0	...
G056.2739+00.5889	SSTGLMC G056.2739+00.5889	293.44110	20.93440	56.8	305.6	748.7	826.5	854.8	2540.8	2852.9	2072.2	1803.7	1002.6	2	6
G058.3473−00.7530	SSTGLMC G058.3470−00.7531	295.79159	22.08230	314.0	817.2	1198.0	587.2	521.4	1377.2	1082.1	443.2	0	2
G058.8901+00.1460	SSTGLMC G058.8899+00.1459	295.23770	22.99950	71.5	286.5	577.5	441.0	389.9	882.6	313.0	1	...
G059.1886+00.1053	SSTGLMC G059.1884+00.1052	295.43670	23.23880	115.7	401.0	917.4	1343.0	456.3	2047.8	3109.2	4709.0	4388.9	4	...
G059.6938−00.7208	SSTGLMC G059.6938−00.7209	296.49040	23.26470	153.9	502.5	858.9	446.4	378.7	838.6	333.8	0	99
G059.8237−00.5357	SSTGLMC G059.8236−00.5361	296.38690	23.46990	2.7	3.4	6.2	10.2	16.4	18.0	72.3	185.2	...	1169.0	3010.2	...	1	−1
G060.5959+00.8388	SSTGLMC G060.5959+00.8387	295.50280	24.82450	613.9	1778.0	2865.0	1487.0	1121.0	2838.8	2821.3	2083.9	2024.5	1190.2	0	99
G061.2659+00.3183	SSTGLMC G061.2657+00.3183	296.36900	25.14590	693.2	1783.0	2671.0	1006.0	815.3	1856.2	1879.9	1248.6	...	598.4	0	98
G061.4816−00.8337	SSTGLMC G061.4818−00.8337	297.58589	24.75030	6.0	49.3	192.6	1548.0	1322.0	712.3	218.9	0	...
G064.9674+00.4695	SSTGLMC G064.9676+00.4696	298.32740	28.41220	2446.0	4698.0	5648.0	1515.0	1512.0	3911.9	4123.1	2478.5	2738.8	1281.0	3	93
G296.6843+00.4515	SSTGLMC G296.6844+00.4513	179.55750	−61.77310	121.6	448.6	944.3	900.6	1078.0	3655.9	3702.8	2660.4	2630.1	1228.2	0	40
G300.0190+00.0418	SSTGLMC G300.0190+00.0422	186.50111	−62.68610	4.0	39.8	145.7	268.7	232.7	259.1	263.6	911.1	1237.4	972.3	...	598.4	1	98
G300.4380+00.8378	SSTGLMC G300.4380+00.8381	187.55410	−61.93120	131.9	460.4	673.5	328.1	254.1	243.4	143.5	64.3	44.3	1	...
G301.0439+00.0582	SSTGLMC G301.0440+00.0576	188.73289	−62.75300	168.6	416.0	537.4	308.8	175.8	151.2	108.5	464.0	56.5	1	...
G301.2519+00.0987	SSTGLMC G301.2523+00.0983	189.19160	−62.72520	82.7	368.0	707.8	456.6	357.5	761.0	354.0	0	7
G301.5260−00.0920	SSTGLMC G301.5261−00.0919	189.76909	−62.93010	29.2	174.5	401.7	517.2	369.2	170.4	78.0	1	...
G302.6334−00.4974	SSTGLMC G302.6334−00.4973	192.19371	−63.36770	4.1	49.3	202.5	642.3	723.1	2205.5	3017.3	2332.0	2450.0	2177.1	0	1
G304.3464−00.2480	SSTGLMC G304.3464−00.2488	195.98561	−63.08560	0.7	14.8	80.2	239.2	367.5	364.7	295.4	148.8	56.4	0	...
G304.7119+00.5805	SSTGLMC G304.7121+00.5805	196.68300	−62.23840	436.6	1015.0	1596.0	1506.0	1090.0	597.7	278.9	0	42
G304.9706+00.2857	SSTGLMC G304.9703+00.2860	197.28060	−62.51610	39.6	220.8	487.0	...	409.3	395.4	298.1	775.7	987.2	544.5	0	−1
G307.9560+00.2410	SSTGLMC G307.9560+00.2416	203.68510	−62.20760	68.6	282.3	493.3	758.4	714.3	341.0	384.4	1	29
G308.2943−00.3147	SSTGLMC G308.2941−00.3147	204.61480	−62.69600	2.2	36.4	174.2	855.0	926.6	473.4	...	918.2	...	1138.8	1	8
G308.6295−00.2783	SSTGLMC G308.6293−00.2782	205.31670	−62.59770	31.1	280.9	...	893.8	970.9	1940.8	3092.1	3280.1	2640.6	2882.7	3	...
G308.9450−00.2261	SSTGLMC G308.9452−00.2265	205.96529	−62.48440	...	1.5	16.5	238.5	323.1	414.0	389.1	161.8	460.1	1	...
G309.0366+00.1775	SSTGLMC G309.0363+00.1771	205.98281	−62.07050	378.8	...	548.6	544.9	259.4	255.6	1	...
G309.5524−00.1886	SSTGLMC G309.5526−00.1883	207.22969	−62.31930	1421.0	1308.0	741.2	...	993.2	...	523.9	0	...
G309.8575−00.5552	SSTGLMC G309.8576−00.5555	208.05240	−62.60710	0.5	16.7	103.7	1157.0	1286.0	579.8	...	764.8	...	1111.4	1	...
G309.8885−00.3600	SSTGLMC G309.8883−00.3604	208.01909	−62.41011	1.7	44.3	217.5	830.0	832.4	372.1	635.2	344.9	0	...
G310.0299+00.2683	SSTGLMC G310.0300+00.2682	208.00060	−61.76600	...	11.1	70.5	165.5	159.7	184.6	158.0	286.2	218.2	1	...
G310.2791+00.8517	SSTGLMC G310.2791+00.8515	208.22180	−61.14050	65.9	330.1	755.7	763.8	656.5	1432.0	1894.1	1463.4	...	656.2	0	86
G310.3854+00.9975	SSTGLMC G310.3856+00.9973	208.36390	−60.97360	11.7	101.5	262.5	1056.0	1101.0	419.8	354.0	0	−1
G310.4040−00.0968	SSTGLMC G310.4041−00.0974	208.95749	−62.03090	5.4	85.6	305.0	637.8	559.1	266.4	489.7	1	...
G310.6924+00.5680	SSTGLMC G310.6925+00.5675	209.19791	−61.31510	597.7	673.3	2008.1	2443.8	2254.9	2141.1	1796.6	1	13
G310.9407−00.2595	SSTGLMC G310.9412−00.2596	210.15299	−62.05090	8.1	390.2	...	1129.0	1164.0	549.4	...	804.0	...	560.6	1	...
G311.1065+00.7887	SSTGLMC G311.1068+00.7883	209.91080	−60.99591	12.6	139.2	467.2	498.2	466.4	1005.7	1489.4	835.0	...	694.0	1	−1
G311.4028+00.6563	SSTGLMC G311.4033+00.6562	210.57291	−61.04470	...	36.4	171.7	256.1	248.1	285.5	228.8	514.9	262.1	0	...
G311.8197−00.0661	SSTGLMC G311.8202−00.0661	211.82900	−61.62170	21.0	1147.0	844.0	327.6	112.2	0	...
G311.9494+00.3424	SSTGLMC G311.9498+00.3423	211.84119	−61.19300	...	0.9	6.7	125.3	329.5	672.5	906.0	438.1	...	1076.1	2334.7	2250.8	1	21
G312.1156−00.3749	SSTGLMC G312.1163−00.3752	212.61830	−61.82940	7.7	1283.0	1464.0	762.2	1183.8	1388.0	...	1346.3	2	27
G312.6337−00.8068	SSTGLMC G312.6344−00.8070	213.95101	−62.07900	98.2	382.9	671.6	...	330.6	289.6	228.7	466.4	190.0	1	...
G312.9457+00.2002	SSTGLMC G312.9459+00.1998	213.89520	−61.02500	1452.0	1007.0	531.6	163.1	0	...
G313.1766+00.8951	SSTGLMC G313.1768+00.8950	213.88860	−60.29280	325.1	318.1	232.9	517.5	0	...
G313.1902−00.2458	SSTGLMC G313.1907−00.2459	214.67620	−61.36740	1.8	36.3	181.9	1123.0	799.4	361.9	115.5	0	...
G314.2827−00.1505	SSTGLMC G314.2828−00.1516	216.73161	−60.90050	1.3	28.7	155.4	418.1	...	546.2	457.1	229.7	209.4	1	...
G314.6557+00.0915	SSTGLMC G314.6559+00.0909	217.26190	−60.53920	2.9	64.7	296.4	892.5	727.4	368.3	404.5	330.9	0	...
G315.1557−00.3837	SSTGLMC G315.1556−00.3840	218.57280	−60.79100	2.9	14.5	73.8	578.8	411.9	175.7	71.3	0	...

Table 2—Continued

MSX source name	GLIMPSE source name	Coordinates		2MASS				IRAC				MSX			MIPS	MSX Σ var ^a	IRAS Var
		α (J2000) °	δ (J2000) °	F _J mJy	F _H mJy	F _{K_s} mJy	F _{3.6} mJy	F _{4.5} mJy	F _{5.8} mJy	F _{8.0} mJy	F _{8.28} mJy	F _{12.13} mJy	F _{14.65} mJy	F _{21.3} mJy	F ₂₄ mJy		
G315.4204+00.0088	SSTGLMC G315.4206+00.0082	218.75980	-60.32650	1.2	2.4	18.8	1835.0	1514.0	571.2	558.5	601.0	...	402.7	0	...
G315.5231+00.4516	SSTGLMC G315.5233+00.4512	218.60530	-59.87850	1363.0	1161.0	636.8	1049.4	293.4	0	...
G315.7573-00.9574	SSTGLMC G315.7572-00.9576	220.17840	-61.07850	186.6	812.6	1601.0	908.5	750.0	1726.1	2107.4	1338.7	0	80
G315.7636-00.0579	SSTGLMC G315.7638-00.0585	219.44950	-60.25280	...	5.6	52.0	376.9	...	681.0	695.8	351.8	594.2	483.4	...	702.7	0	...
G315.7814+00.4338	SSTGLMC G315.7820+00.4341	219.09260	-59.79420	2.7	30.9	133.8	603.6	452.7	212.8	48.1	0	...
G315.8439+00.0436	SSTGLMC G315.8441+00.0430	219.51611	-60.12760	9.6	142.8	470.7	551.3	423.3	170.5	80.1	0	...
G316.0769-00.7927	SSTGLMC G316.0768-00.7925	220.63840	-60.79680	140.0	564.8	1123.0	1438.0	982.3	505.4	257.9	0	...
G316.3803-00.9495	SSTGLMC G316.3801-00.9501	221.33770	-60.81190	54.2	221.0	420.3	255.9	182.6	181.4	152.3	310.2	105.4	0	...
G317.2744+00.9946	SSTGLMC G317.2746+00.9947	221.30790	-58.67191	62.7	167.5	259.9	255.6	193.3	161.2	147.8	281.3	69.8	0	...
G317.4117-00.6888	SSTGLMC G317.4110-00.6887	222.99069	-60.12780	15.5	125.9	330.5	298.4	195.0	194.3	134.6	241.8	84.8	0	...
G317.4728-00.8832	SSTGLMC G317.4723-00.8828	223.27620	-60.27410	101.0	380.8	680.3	377.0	298.1	295.5	321.8	826.3	1098.4	703.0	0	...
G318.2479-00.9418	SSTGLMC G318.2478-00.9417	224.71150	-59.96949	190.2	937.3	1886.0	897.3	825.6	2378.6	2978.1	2138.1	...	1043.6	0	...
G318.7614-00.2781	SSTGLMC G318.7610-00.2777	224.98751	-59.14210	9.3	85.0	266.6	...	353.0	347.1	291.1	638.6	510.8	0	...
G318.9134+00.7526	SSTGLMC G318.9131+00.7530	224.31650	-58.16030	40.9	202.8	520.4	154.3	257.4	313.7	490.2	1518.8	1804.1	1638.3	...	1022.7	1	...
G318.9816+00.7677	SSTGLMC G318.9813+00.7679	224.41760	-58.11530	62.3	287.8	660.0	813.8	718.3	1700.9	2204.7	1384.3	...	1090.6	0	...
G319.1733+00.4665	SSTGLMC G319.1735+00.4667	225.00729	-58.29110	778.4	732.9	277.1	132.4	1	...
G319.2663-00.4101	SSTGLMC G319.2662-00.4097	225.97289	-59.01570	1562.0	1419.0	478.5	181.1	0	...
G319.3346+00.6077	SSTGLMC G319.3345+00.6080	225.14950	-58.09030	30.1	149.5	302.5	479.7	352.1	182.8	118.9	0	...
G319.7738+00.4793	SSTGLMC G319.7735+00.4799	225.99360	-57.99159	27.5	148.3	356.7	288.5	241.6	256.9	325.4	1146.2	1645.6	1090.3	...	973.7	0	45
G319.8400+00.0308	SSTGLMC G319.8394+00.0312	226.51959	-58.35020	82.2	480.3	1127.0	1458.0	1535.0	3938.5	4439.8	2854.2	2638.4	1002.4	0	0
G320.2584+00.8760	SSTGLMC G320.2585+00.8761	226.42140	-57.40850	0.6	10.7	87.7	347.3	445.5	601.6	791.6	1827.7	2351.6	1987.8	...	787.0	2	-1
G320.5274+00.7643	SSTGLMC G320.5277+00.7641	226.95760	-57.37230	32.7	128.4	225.1	205.9	165.8	148.6	110.9	227.8	67.1	0	...
G321.3065+00.2253	SSTGLMC G321.3070+00.2255	228.71201	-57.43840	14.3	45.0	81.0	283.1	342.9	426.8	401.7	115.7	85.3	0	...
G321.7691-00.8164	SSTGLMC G321.7693-00.8164	230.48531	-58.07410	10.1	68.3	177.5	267.3	230.3	258.4	264.2	623.0	316.6	0	0
G321.9739-00.5701	SSTGLMC G321.9740-00.5702	230.55670	-57.75600	19.0	118.3	302.2	582.7	445.5	233.6	143.6	0	...
G321.9984+00.2483	SSTGLMC G321.9987+00.2483	229.77550	-57.05360	...	152.3	160.2	280.6	252.8	269.5	261.5	568.6	411.4	0	...
G322.1414+00.9054	SSTGLMC G322.1415+00.9055	229.35890	-56.42110	2.8	38.0	172.3	998.8	1101.0	573.9	614.7	0	...
G322.1744+00.0134	SSTGLMC G322.1748+00.0135	230.28131	-57.15700	8.5	84.2	302.2	1279.0	1520.0	704.1	...	927.8	...	1713.7	1	97
G322.3099-00.2316	SSTGLMC G322.3101-00.2317	230.73760	-57.28910	5.7	72.1	324.1	1627.0	1294.0	710.6	198.6	0	...
G322.3847+00.5335	SSTGLMC G322.3848+00.5333	230.09160	-56.60560	43.3	179.6	301.5	348.0	135.8	606.6	0	...
G322.4192-00.0746	SSTGLMC G322.4196-00.0744	230.74821	-57.09780	54.1	342.5	792.0	437.6	325.8	350.8	322.2	816.8	491.0	0	...
G323.2785+00.0493	SSTGLMC G323.2794+00.0492	231.92971	-56.51870	0.7	14.8	87.8	806.6	906.1	329.4	479.6	1	-1
G323.6836+00.9627	SSTGLMC G323.6836+00.9624	231.61700	-55.53490	52.2	184.1	340.4	402.3	310.0	339.4	347.9	935.2	1030.0	584.4	0	98
G323.7987-00.0435	SSTGLMC G323.7996-00.0444	232.79991	-56.30080	3.4	85.6	256.0	520.6	656.6	317.8	1908.2	1	...
G324.2129+00.6429	SSTGLMC G324.2130+00.6428	232.70740	-55.50060	125.8	479.0	1103.0	1088.0	1084.0	2790.7	3358.6	2328.1	...	1214.2	1	28
G325.5458-00.3432	SSTGLMC G325.5463-00.3436	235.63550	-55.51560	98.0	441.7	793.5	409.6	390.0	344.2	308.1	617.6	269.1	0	...
G325.6836-00.0080	SSTGLMC G325.6842-00.0078	235.47289	-55.16520	51.4	310.1	723.0	1187.0	918.2	484.8	356.2	0	...
G326.3422-00.6056	SSTGLMC G326.3428-00.6056	237.02640	-55.23540	3.8	72.3	319.7	1084.0	785.1	373.3	188.8	1	...
G326.5913+00.1750	SSTGLMC G326.5915+00.1752	236.52961	-54.46740	67.5	1264.0	1258.0	437.6	1288.8	0	99
G326.9617+00.4398	SSTGLMC G326.9621+00.4395	236.75000	-54.03070	...	9.3	60.5	404.2	...	793.1	849.5	338.4	477.8	0	1
G327.0069-00.1135	SSTGLMC G327.0073-00.1132	237.39821	-54.43660	...	5.9	96.7	1350.0	1123.0	390.8	...	666.5	...	689.0	0	...
G327.2580+00.6483	SSTGLMC G327.2582+00.6479	236.92641	-53.68370	17.8	207.2	657.0	1014.0	642.2	332.5	145.6	0	...
G327.4016+00.0136	SSTGLMC G327.4020+00.0136	237.78860	-54.09020	6.9	96.2	406.9	1772.0	1464.0	764.8	1086.4	898.5	...	787.3	1	...
G327.5752-00.9163	SSTGLMC G327.5756-00.9162	239.03390	-54.69800	26.6	125.6	294.3	428.7	313.5	286.3	253.7	620.0	0	...
G327.6759+00.8157	SSTGLMC G327.6760+00.8153	237.30210	-53.29290	11.1	339.4	...	783.8	637.9	313.2	168.1	0	...
G327.6830+00.0870	SSTGLMC G327.6832+00.0869	238.08150	-53.85590	...	6.8	67.3	250.6	364.0	545.2	579.1	283.5	895.5	0	...
G327.8912+00.8528	SSTGLMC G327.8912+00.8523	237.54409	-53.12950	...	0.8	14.8	281.0	...	879.2	867.0	424.3	186.7	0	...
G328.1669+00.3143	SSTGLMC G328.1671+00.3143	238.46949	-53.37340	3.7	407.1	...	1596.0	1461.0	596.8	...	933.5	...	1221.8	1	...
G328.3125-00.2136	SSTGLMC G328.3127-00.2133	239.22630	-53.68580	17.9	212.8	712.4	1639.0	1088.0	483.9	226.2	1	...

Table 2—Continued

MSX source name	GLIMPSE source name	Coordinates		2MASS			IRAC					MSX			MIPS	MSX Σ var ^a	IRAS Var
		α (J2000) °	δ (J2000) °	F _J mJy	F _H mJy	F _{K_s} mJy	F _{3.6} mJy	F _{4.5} mJy	F _{5.8} mJy	F _{8.0} mJy	F _{8.28} mJy	F _{12.13} mJy	F _{14.65} mJy	F _{21.3} mJy	F ₂₄ mJy		
G328.3644+00.3438	SSTGLMC G328.3647+00.3434	238.69280	-53.22470	...	1.0	29.0	409.3	...	1658.0	1533.0	405.0	...	1068.1	...	2128.8	0	28
G328.9432+00.9410	SSTGLMC G328.9439+00.9417	238.79799	-52.39560	...	11.6	74.3	441.5	...	608.2	411.8	202.7	64.1	1	...
G329.0542+00.0576	SSTGLMC G329.0549+00.0575	239.87860	-52.99880	...	10.9	86.1	1153.0	795.8	318.9	118.1	0	...
G329.1594-00.7949	SSTGLMC G329.1598-00.7944	240.94790	-53.57261	13.1	288.9	...	946.6	1028.0	457.3	587.2	0	...
G329.2989-00.1228	SSTGLMC G329.2995-00.1229	240.38220	-52.97541	41.0	253.0	556.6	510.2	355.4	188.6	62.2	1	...
G329.7937-00.0149	SSTGLMC G329.7941-00.0148	240.87981	-52.56820	5.8	87.0	373.9	1611.0	1085.0	559.2	216.1	0	...
G329.8000-00.4921	SSTGLMC G329.8003-00.4920	241.41130	-52.92070	...	2.9	21.8	388.0	...	1050.0	1168.0	471.3	324.9	1	...
G329.9308-00.2980	SSTGLMC G329.9310-00.2982	241.35850	-52.68871	44.4	286.8	676.6	424.7	348.1	375.5	309.0	813.7	530.0	0	...
G329.9730-00.0905	SSTGLMC G329.9733-00.0909	241.18290	-52.50581	...	9.0	130.1	1897.0	1324.0	692.9	300.1	0	...
G330.0338+00.0399	SSTGLMC G330.0340+00.0400	241.11510	-52.36790	13.8	339.2	...	689.1	514.8	220.0	121.2	1	...
G330.0671-00.8481	SSTGLMC G330.0675-00.8479	242.13670	-53.00550	17.0	98.8	243.0	474.6	621.4	1285.1	1582.1	1579.0	...	1194.2	0	1
G330.2280+00.4417	SSTGLMC G330.2282+00.4414	240.91800	-51.93830	1.8	37.6	169.5	188.5	165.1	205.6	168.1	468.9	377.6	0	...
G330.2594+00.2857	SSTGLMC G330.2596+00.2858	241.12411	-52.03430	...	2.7	39.3	733.9	603.3	306.4	399.6	1	...
G330.5727-00.6220	SSTGLMC G330.5728-00.6218	242.49930	-52.49690	24.8	158.7	372.2	258.7	217.1	239.0	214.8	455.7	316.1	1	28
G330.6676+00.7175	SSTGLMC G330.6675+00.7172	241.15360	-51.44040	0.9	14.8	70.1	423.2	...	906.1	1142.0	627.8	...	1164.0	...	991.2	1	...
G330.8496-00.4309	SSTGLMC G330.8497-00.4305	242.61960	-52.16870	11.4	194.4	755.7	2030.0	1429.0	746.2	...	921.5	...	815.1	2	...
G331.0967-00.6433	SSTGLMC G331.0967-00.6432	243.15040	-52.15540	7.3	23.8	67.9	187.5	219.9	185.1	168.6	484.8	...	1954.2	2970.2	...	0	-1
G331.2336+00.2627	SSTGLMC G331.2332+00.2628	242.31590	-51.39829	...	16.6	148.8	1509.0	1112.0	440.1	340.5	1	...
G331.3052-00.4972	SSTGLMC G331.3051-00.4969	243.23440	-51.90620	...	1.8	5.5	44.6	182.0	585.4	1009.0	2077.2	3199.7	2965.1	2037.3	1226.0	0	...
G331.3892+00.7251	SSTGLMC G331.3890+00.7245	242.00140	-50.95210	9.4	93.3	304.7	734.9	569.0	267.1	189.9	0	-1
G331.4605+00.3007	SSTGLMC G331.4605+00.3006	242.54180	-51.21670	2.4	52.2	252.5	1480.0	1280.0	556.3	524.0	1	...
G331.5816+00.3472	SSTGLMC G331.5812+00.3471	242.63310	-51.10030	7.2	279.1	...	854.7	791.7	373.2	211.7	0	...
G331.8045+00.9764	SSTGLMC G331.8047+00.9762	242.21810	-50.48650	1.5	19.1	71.4	384.4	388.5	401.1	387.0	183.8	0	...
G331.8074+00.1909	SSTGLMC G331.8072+00.1911	243.06560	-51.06080	...	1.5	41.1	376.7	...	1041.0	911.6	516.5	...	827.0	...	668.3	1	...
G331.9057-00.6572	SSTGLMC G331.9051-00.6568	244.11510	-51.60780	11.2	67.3	206.0	400.2	449.8	507.5	558.0	1280.7	1618.9	1218.7	...	921.9	1	...
G332.2506+00.5480	SSTGLMC G332.2505+00.5475	243.19000	-50.49710	1032.0	993.5	489.3	434.6	0	...
G332.9649-00.9356	SSTGLMC G332.9647-00.9354	245.63580	-51.06320	22.4	119.8	291.3	830.7	825.9	431.0	1	...
G333.0143-00.1582	SSTGLMC G333.0136-00.1581	244.82471	-50.47690	5.7	161.4	783.3	2038.0	959.6	329.5	106.4	0	...
G333.1157-00.9108	SSTGLMC G333.1153-00.9108	245.77680	-50.93870	39.1	342.2	977.1	1281.0	1155.0	631.8	0	...
G333.2359+00.9859	SSTGLMC G333.2356+00.9861	243.83300	-49.50130	...	5.0	31.8	378.9	...	1000.0	1126.0	334.7	0	...
G333.3106-00.7228	SSTGLMC G333.3106-00.7227	245.78260	-50.66789	58.7	416.8	1013.0	617.0	536.0	1025.4	1469.2	804.1	...	1055.7	1	...
G333.6438+00.6955	SSTGLMC G333.6437+00.6954	244.59480	-49.42650	2.0	46.5	225.1	1192.0	1072.0	499.8	842.5	781.0	0	...
G333.7236+00.5406	SSTGLMC G333.7235+00.5403	244.84930	-49.48130	672.5	489.4	237.3	244.9	0	...
G333.7973+00.0482	SSTGLMC G333.7969+00.0484	245.46530	-49.77900	5.6	244.3	...	1192.0	1158.0	434.4	537.5	0	...
G333.9966+00.7190	SSTGLMC G333.9969+00.7191	244.95560	-49.16260	5.6	67.7	258.4	881.2	913.7	348.5	...	641.7	...	414.5	0	...
G334.0970-00.3297	SSTGLMC G334.0969-00.3297	246.20830	-49.83200	...	22.2	155.6	1029.0	863.5	417.4	906.4	356.1	0	...
G334.3924-00.7850	SSTGLMC G334.3929-00.7852	247.03460	-49.93690	16.2	82.7	170.6	205.7	161.2	160.5	161.9	358.3	201.3	0	...
G334.4668+00.9687	SSTGLMC G334.4663+00.9689	245.19659	-48.65440	1.7	22.8	105.1	999.4	1049.0	559.2	...	706.1	0	94
G334.5243+00.7274	SSTGLMC G334.5241+00.7275	245.51670	-48.78470	49.2	422.2	1108.0	1229.0	898.5	470.6	261.1	0	...
G334.6799-00.8348	SSTGLMC G334.6802-00.8348	247.39851	-49.76340	44.3	259.6	678.5	702.3	783.9	1786.6	1823.0	1565.3	...	1198.9	0	99
G334.8128-00.1059	SSTGLMC G334.8125-00.1053	246.73030	-49.16300	1.7	54.5	311.0	311.6	...	663.1	755.8	1656.4	2208.5	1917.2	...	1627.8	1	...
G334.9467-00.4008	SSTGLMC G334.9466-00.4005	247.19780	-49.27090	6.4	253.0	...	1248.0	1448.0	392.3	...	964.4	...	2930.0	0	9
G335.4507+00.0785	SSTGLMC G335.4500+00.0789	247.20010	-48.57530	...	1.5	35.9	133.7	270.0	475.3	511.0	1135.6	1899.7	1800.2	...	934.6	2	...
G335.4943-00.6316	SSTGLMC G335.4941-00.6312	248.02930	-49.03130	...	48.2	205.8	763.7	902.2	2615.8	3270.9	2899.2	3080.7	2235.3	0	62
G335.5007+00.3441	SSTGLMC G335.5003+00.3440	246.96309	-48.35540	1.3	31.5	156.4	1125.0	1230.0	534.7	...	923.1	...	595.5	0	...
G335.8384-00.2910	SSTGLMC G335.8377-00.2906	248.00830	-48.54740	...	49.0	208.9	638.2	558.8	265.8	368.4	0	...
G335.9515+00.8287	SSTGLMC G335.9511+00.8287	246.90800	-47.69460	7.7	46.4	132.4	401.6	328.9	352.2	346.4	768.2	617.8	0	...
G336.0412+00.9770	SSTGLMC G336.0410+00.9771	246.84190	-47.52711	47.0	252.8	550.5	441.7	374.0	372.1	351.0	774.3	0	34
G336.0517-00.5214	SSTGLMC G336.0510-00.5213	248.48260	-48.54800	4.9	40.8	134.1	1072.0	1098.0	489.0	...	550.8	...	732.0	0	...

Table 2—Continued

MSX source name	GLIMPSE source name	Coordinates		2MASS			IRAC					MSX			MIPS	MSX $\sum \text{var}^a$	IRAS Var
		α (J2000) °	δ (J2000) °	F _J mJy	F _H mJy	F _{K_s} mJy	F _{3.6} mJy	F _{4.5} mJy	F _{5.8} mJy	F _{8.0} mJy	F _{8.28} mJy	F _{12.13} mJy	F _{14.65} mJy	F _{21.3} mJy	F ₂₄ mJy		
G336.2826−00.7376	SSTGLMC G336.2817−00.7378	248.95900	−48.52410	1.5	23.0	117.5	681.1	493.4	189.3	111.1	0	...
G336.4238−00.5990	SSTGLMC G336.4229−00.5989	248.94810	−48.32650	101.4	565.9	1221.0	734.9	630.6	1480.1	1976.4	1355.3	...	872.4	0	32
G336.5577+00.3704	SSTGLMC G336.5567+00.3706	248.02040	−47.57021	6.9	89.3	330.5	715.0	445.3	181.5	94.4	0	...
G336.6327+00.7960	SSTGLMC G336.6322+00.7962	247.63810	−47.22410	1.4	28.4	160.4	404.6	448.6	544.8	607.0	1473.7	2200.1	1701.0	...	884.2	1	...
G336.7941−00.9962	SSTGLMC G336.7937−00.9969	249.76470	−48.31780	1430.0	1294.0	577.9	406.6	0	0
G336.8535+00.5122	SSTGLMC G336.8529+00.5123	248.16550	−47.25719	...	10.1	56.4	253.8	310.6	415.2	441.5	825.4	1220.9	1037.7	...	862.1	1	−1
G336.8569+00.6024	SSTGLMC G336.8563+00.6026	248.07170	−47.19320	87.1	555.5	1393.0	1375.0	1194.0	2663.8	3656.9	2981.7	3553.2	1705.7	1	...
G336.9322−00.6167	SSTGLMC G336.9314−00.6163	249.47950	−47.96170	25.2	159.3	381.9	426.1	347.0	354.9	275.8	492.0	...	630.1	...	184.7	1	...
G337.0528−00.2264	SSTGLMC G337.0521−00.2258	249.16881	−47.61040	114.0	...	1012.0	941.4	382.4	0	−1
G337.0848−00.5550	SSTGLMC G337.0848−00.5550	249.56320	−47.80700	...	4.4	23.3	42.8	93.8	154.4	247.9	1056.9	1352.3	1475.3	...	1171.8	0	24
G337.1266+00.3575	SSTGLMC G337.1259+00.3580	248.60560	−47.16200	...	2.9	17.5	343.6	...	1333.0	1500.0	453.0	2261.6	0	59
G337.2420+00.1455	SSTGLMC G337.2412+00.1461	248.95040	−47.22010	1.2	2.5	6.6	240.9	...	1110.0	1066.0	293.2	968.4	0	...
G337.5274−00.6458	SSTGLMC G337.5273−00.6458	250.10130	−47.53710	204.6	1112.0	2265.0	1522.0	1308.0	650.7	957.2	0	...
G337.5330−00.7144	SSTGLMC G337.5331−00.7143	250.18300	−47.57840	13.8	126.6	391.1	826.9	759.7	295.8	497.6	0	...
G337.5482+00.5897	SSTGLMC G337.5482+00.5897	248.77289	−46.69440	18.5	144.9	373.9	...	334.2	453.2	322.5	743.8	491.7	0	25
G337.5909+00.0598	SSTGLMC G337.5910+00.0600	249.38819	−47.01930	1.0	24.1	124.0	...	408.5	543.0	394.8	766.2	...	1081.2	...	549.7	1	...
G337.6931−00.4936	SSTGLMC G337.6926−00.4939	250.09529	−47.31220	2.5	45.1	190.3	378.0	433.9	402.3	435.2	174.4	461.6	0	...
G337.8933+00.7975	SSTGLMC G337.8925+00.7978	248.88880	−46.29960	33.3	132.5	240.9	168.1	107.8	110.4	82.7	154.7	59.6	0	...
G337.9022+00.4250	SSTGLMC G337.9023+00.4253	249.29740	−46.54350	245.7	314.6	368.6	403.3	932.8	...	937.1	...	711.0	0	...
G337.9437−00.2436	SSTGLMC G337.9431−00.2435	250.06480	−46.95880	139.7	376.5	673.0	656.2	275.3	...	561.5	...	497.9	1	...
G338.0102+00.4628	SSTGLMC G338.0104+00.4631	249.36170	−46.43800	6.4	64.0	192.8	415.1	431.2	479.0	481.1	228.7	177.0	0	...
G338.0432−00.1512	SSTGLMC G338.0435−00.1512	250.06020	−46.82300	21.0	219.9	657.5	1191.0	811.1	356.5	194.6	0	...
G338.1223+00.2171	SSTGLMC G338.1220+00.2173	249.73600	−46.51900	28.9	210.4	620.5	876.9	845.6	2412.2	2713.1	2213.2	2611.8	1742.9	2	13
G338.2051−00.3526	SSTGLMC G338.2049−00.3525	250.43740	−46.83490	29.4	282.3	841.7	1467.0	1346.0	615.9	867.2	772.3	1271.4	580.5	0	...
G338.3019−00.1298	SSTGLMC G338.3012−00.1295	250.28669	−46.61510	...	9.8	118.0	1190.0	889.0	236.1	...	385.7	...	469.2	1	...
G338.4481+00.4598	SSTGLMC G338.4487+00.4605	249.78830	−46.11430	19.8	101.0	237.4	329.2	286.1	294.7	273.2	564.3	289.5	1	...
G338.5139−00.9458	SSTGLMC G338.5140−00.9456	251.38961	−46.99060	27.6	156.6	309.0	288.8	244.0	261.9	227.8	427.1	217.1	0	...
G338.5368+00.2463	SSTGLMC G338.5365+00.2468	250.10370	−46.18990	102.6	504.8	1091.0	781.1	959.4	2280.0	2932.7	2382.4	2500.1	1265.9	1	...
G338.5735−00.4072	SSTGLMC G338.5733−00.4073	250.85100	−46.59350	...	7.6	61.7	1116.0	853.9	432.2	123.4	1	...
G338.6715−00.1221	SSTGLMC G338.6713−00.1221	250.63250	−46.33220	7.6	144.6	575.9	1739.0	1316.0	667.6	...	752.2	...	420.9	1	...
G338.7111−00.4644	SSTGLMC G338.7109−00.4648	251.04490	−46.52701	44.5	408.7	...	790.2	530.4	208.6	258.8	1	...
G338.7428−00.7448	SSTGLMC G338.7421−00.7450	251.38430	−46.68590	13.0	140.1	459.5	1228.0	1294.0	662.7	1463.3	0	...
G338.7552+00.6664	SSTGLMC G338.7552+00.6663	249.86060	−45.74760	806.9	837.0	2068.0	2758.4	2255.9	2652.0	1069.2	0	...
G338.8028+00.7322	SSTGLMC G338.8027+00.7321	249.83560	−45.66830	1.8	19.7	93.4	1330.0	1514.0	618.3	826.6	0	...
G338.8601−00.7865	SSTGLMC G338.8600−00.7871	251.54150	−46.62390	301.8	1136.0	2128.0	1532.0	1063.0	531.3	1311.3	342.8	0	...
G339.2514−00.3656	SSTGLMC G339.2511−00.3650	251.44670	−46.05300	...	4.7	45.1	1053.0	847.2	202.7	455.8	1	...
G339.4448+00.8592	SSTGLMC G339.4445+00.8594	250.30669	−45.10380	178.7	911.0	2025.0	297.5	...	1942.0	1531.0	775.6	937.0	0	93
G339.5353−00.0529	SSTGLMC G339.5348−00.0524	251.37099	−45.63400	155.7	406.7	879.0	941.7	496.4	...	723.7	...	302.6	1	...
G339.5589+00.2363	SSTGLMC G339.5587+00.2368	251.08010	−45.42730	26.3	155.0	445.8	997.3	1095.0	3506.7	4925.7	4033.9	4545.2	...	2	...
G339.5698−00.6387	SSTGLMC G339.5698−00.6385	252.04319	−45.98730	3.8	48.2	195.3	942.4	1044.0	533.4	930.4	867.7	...	1173.1	0	3
G339.5712−00.1572	SSTGLMC G339.5708−00.1566	251.51770	−45.67450	2.2	45.2	216.9	436.0	...	763.7	700.9	287.5	323.4	1	...
G339.5762−00.6655	SSTGLMC G339.5762−00.6651	252.07860	−45.99970	7.6	75.3	251.6	897.1	789.2	416.3	379.4	0	...
G339.8957−00.5130	SSTGLMC G339.8954−00.5128	252.20640	−45.65710	23.3	1467.0	1374.0	459.0	...	774.7	...	860.8	1	...
G339.9862−00.1270	SSTGLMC G339.9861−00.1262	251.86880	−45.33900	...	13.2	97.2	1052.0	805.7	351.2	460.5	1	...
G340.2393−00.6684	SSTGLMC G340.2393−00.6681	252.69140	−45.49290	27.7	232.2	681.0	647.5	604.5	1375.8	1869.4	1283.7	...	1194.2	0	...
G340.3852+00.7799	SSTGLMC G340.3856+00.7798	251.26070	−44.44650	...	3.1	29.8	208.4	268.3	390.0	486.1	1282.4	1737.8	1512.2	...	591.3	1	...
G340.4449+00.0403	SSTGLMC G340.4448+00.0410	252.10700	−44.88060	633.9	492.7	195.8	198.8	0	...
G340.5787+00.2826	SSTGLMC G340.5787+00.2829	251.96770	−44.62200	...	1.9	13.0	276.3	426.9	581.9	623.9	263.5	362.5	1	...
G340.6621+00.6965	SSTGLMC G340.6619+00.6968	251.60120	−44.29050	52.4	232.4	466.4	471.3	440.8	1064.8	1020.2	406.4	0	...

Table 2—Continued

MSX source name	GLIMPSE source name	Coordinates		2MASS			IRAC					MSX			MIPS	MSX Σ var ^a	IRAS Var
		α (J2000) °	δ (J2000) °	F _J mJy	F _H mJy	F _{K_s} mJy	F _{3.6} mJy	F _{4.5} mJy	F _{5.8} mJy	F _{8.0} mJy	F _{8.28} mJy	F _{12.13} mJy	F _{14.65} mJy	F _{21.3} mJy	F ₂₄ mJy		
G340.6811−00.4358	SSTGLMC G340.6812−00.4355	252.83720	−45.00429	18.6	188.4	530.6	...	372.2	389.6	277.4	645.8	846.8	791.4	...	373.8	0	...
G340.8303−00.2953	SSTGLMC G340.8303−00.2953	252.81870	−44.79980	0.4	15.3	107.4	952.7	838.2	290.8	771.8	0	...
G340.8423+00.1797	SSTGLMC G340.8425+00.1801	252.31630	−44.48660	...	13.4	99.5	820.7	707.4	328.8	362.9	0	...
G340.9568−00.5105	SSTGLMC G340.9567−00.5101	253.16629	−44.83910	...	12.2	74.9	281.7	373.1	439.0	397.6	141.6	228.6	0	...
G341.0395−00.9624	SSTGLMC G341.0392−00.9622	253.73510	−45.06030	21.0	282.5	...	803.2	875.0	445.5	1216.9	1	...
G341.1707−00.8409	SSTGLMC G341.1706−00.8410	253.71830	−44.88190	4.2	59.4	214.9	220.5	209.3	216.8	205.0	493.2	365.5	0	...
G341.4614+00.4538	SSTGLMC G341.4616+00.4545	252.57630	−43.83570	13.8	135.0	406.9	682.0	462.5	221.5	111.8	0	...
G341.4846+00.7134	SSTGLMC G341.4847+00.7133	252.32110	−43.65150	3.9	41.6	143.5	439.8	429.4	440.3	407.9	216.8	300.4	1	...
G341.5689+00.9575	SSTGLMC G341.5690+00.9577	252.13789	−43.43000	4.9	45.3	183.3	1316.0	1252.0	631.8	335.6	0	−1
G341.6093−00.8796	SSTGLMC G341.6092−00.8794	254.14770	−44.56451	37.4	257.0	689.8	...	433.5	465.9	444.4	1463.1	1763.6	1699.9	...	1229.7	0	93
G341.6311−00.8481	SSTGLMC G341.6313−00.8480	254.13231	−44.52780	7.7	73.9	218.1	257.9	217.6	230.6	219.8	540.9	466.0	0	0
G341.6516−00.9705	SSTGLMC G341.6517−00.9706	254.28440	−44.58820	19.5	114.3	271.8	299.7	237.8	239.9	241.1	678.7	307.3	0	...
G341.7674+00.2533	SSTGLMC G341.7677+00.2534	253.06050	−43.72780	403.6	446.2	526.2	413.0	206.6	202.2	0	...
G341.7774+00.8956	SSTGLMC G341.7774+00.8958	252.38751	−43.31010	2.1	20.2	91.7	764.1	729.2	352.5	672.1	1	...
G341.9257−00.7920	SSTGLMC G341.9252−00.7917	254.32829	−44.26260	20.0	165.6	442.9	306.3	277.5	314.9	291.9	689.4	463.3	1	...
G342.2673+00.1098	SSTGLMC G342.2674+00.1097	253.65040	−43.43130	...	8.1	73.2	1130.0	933.8	475.7	414.5	1	...
G342.3173+00.8952	SSTGLMC G342.3171+00.8955	252.86050	−42.89520	640.0	673.4	1624.4	2092.8	1917.7	...	1912.2	0	98
G342.3343−00.1724	SSTGLMC G342.3341−00.1723	254.01120	−43.55650	1.6	36.6	121.1	336.4	521.5	1465.2	2139.3	2565.0	2369.0	1575.4	1	62
G342.5349+00.6807	SSTGLMC G342.5349+00.6812	253.27530	−42.86340	678.4	740.6	360.4	397.9	0	...
G342.5501−00.0093	SSTGLMC G342.5502−00.0090	254.02230	−43.28610	0.8	21.6	121.9	834.9	702.7	330.2	322.6	0	...
G342.6239+00.1942	SSTGLMC G342.6240+00.1943	253.86809	−43.10090	5.6	263.8	...	1096.0	1097.0	467.1	...	729.3	...	919.5	1	...
G342.6732+00.3256	SSTGLMC G342.6730+00.3260	253.77060	−42.98010	171.8	438.4	789.4	905.4	453.2	495.6	0	...
G342.6768+00.3646	SSTGLMC G342.6768+00.3646	253.73220	−42.95270	42.3	401.7	1142.0	1714.0	1508.0	810.4	1421.9	1333.4	1	90
G342.7817−00.6938	SSTGLMC G342.7819−00.6937	254.95830	−43.53040	...	2.8	24.4	1306.0	1413.0	381.3	1139.1	0	0
G342.8067−00.2514	SSTGLMC G342.8066−00.2512	254.50190	−43.23670	...	1.2	15.9	1965.0	1576.0	854.6	...	941.4	...	639.5	0	...
G342.9028−00.1444	SSTGLMC G342.9024−00.1442	254.46890	−43.09480	134.0	...	1098.0	1179.0	510.0	...	829.3	...	1079.2	1	...
G342.9246+00.5858	SSTGLMC G342.9245+00.5861	253.71029	−42.62090	9.5	110.7	402.1	1594.0	1426.0	735.7	461.6	0	...
G343.0279−00.7203	SSTGLMC G343.0278−00.7206	255.19610	−43.35291	25.7	135.4	458.4	785.5	1790.9	2463.0	2313.8	1908.7	1293.9	2	97
G343.1116−00.9398	SSTGLMC G343.1114−00.9401	255.50520	−43.42150	6.6	406.2	...	1340.0	1571.0	749.9	...	1094.7	...	1710.2	1	11
G343.1639−00.8416	SSTGLMC G343.1639−00.8418	255.44241	−43.32010	898.2	1031.0	2766.1	4118.9	3585.7	3089.9	1625.1	0	99
G343.3880+00.3509	SSTGLMC G343.3881+00.3512	254.35250	−42.40680	320.5	...	741.0	596.1	287.5	150.1	1	...
G343.5526+00.3705	SSTGLMC G343.5523+00.3707	254.47030	−42.26570	4.5	70.3	356.4	842.5	702.4	1905.7	2485.7	2063.9	1780.9	890.6	0	...
G343.5640−00.4805	SSTGLMC G343.5639−00.4805	255.38800	−42.78260	1.5	53.3	300.0	1307.0	1218.0	666.9	1229.4	1023.3	...	1019.3	1	0
G343.6183+00.0785	SSTGLMC G343.6180+00.0787	254.83520	−42.39540	1.5	34.9	209.5	1434.0	1247.0	630.7	639.0	0	...
G343.6554−00.8070	SSTGLMC G343.6548−00.8069	255.81650	−42.90990	42.2	280.5	658.8	886.0	673.9	342.0	234.4	0	...
G343.7460−00.5851	SSTGLMC G343.7460−00.5851	255.65221	−42.70270	2.6	88.6	269.4	665.8	847.0	2124.2	3254.1	3590.1	3407.6	1695.1	1	98
G343.7577−00.9670	SSTGLMC G343.7576−00.9670	256.07480	−42.92610	6.5	62.2	196.4	295.2	305.6	346.1	413.3	1095.4	1952.0	1069.0	1812.0	1270.2	0	92
G343.9112−00.7970	SSTGLMC G343.9113−00.7967	256.01791	−42.70090	7.2	24.1	45.0	232.2	354.7	482.1	471.1	141.4	81.0	0	...
G343.9540−00.3317	SSTGLMC G343.9537−00.3316	255.55270	−42.38320	...	2.5	47.1	1248.0	1131.0	617.3	912.8	960.8	...	1015.5	1	0
G344.0593+00.2917	SSTGLMC G344.0592+00.2921	254.97679	−41.91690	96.0	419.5	739.1	...	398.3	381.9	365.6	892.8	...	1163.5	...	399.9	1	...
G344.1673−00.3396	SSTGLMC G344.1670−00.3394	255.73751	−42.21920	0.9	21.0	110.9	202.4	209.9	243.4	234.0	578.8	791.6	493.3	0	−1
G344.2219+00.8415	SSTGLMC G344.2217+00.8416	254.53360	−41.44870	38.3	246.8	587.1	485.9	440.8	1012.3	1334.7	436.5	0	...
G344.2898−00.0247	SSTGLMC G344.2894−00.0245	255.50270	−41.92979	3.0	165.9	1108.0	2243.0	1371.0	773.4	1035.4	870.4	...	516.5	0	−1
G344.2899−00.8839	SSTGLMC G344.2895−00.8837	256.42331	−42.45230	26.6	159.8	375.3	598.0	587.1	234.3	271.9	0	5
G344.5918−00.2070	SSTGLMC G344.5915−00.2071	255.94410	−41.80180	5.0	242.9	...	967.2	1242.0	500.0	2214.5	1	6
G344.7291−00.5689	SSTGLMC G344.7287−00.5691	256.44229	−41.91210	...	5.9	67.2	430.0	443.3	550.6	431.1	992.4	1367.0	1177.4	...	1072.7	0	4
G344.7318−00.8354	SSTGLMC G344.7316−00.8358	256.73070	−42.07050	3.8	43.7	146.8	342.2	565.4	1271.6	1592.4	812.8	0	...
G344.9214+00.1870	SSTGLMC G344.9214+00.1868	255.79480	−41.30040	6.2	86.2	292.6	651.5	467.8	243.3	160.8	0	...
G344.9551−00.1101	SSTGLMC G344.9547−00.1103	256.13639	−41.45440	25.1	262.5	936.6	1416.0	1233.0	2604.8	3870.9	2881.1	3077.3	2697.9	3	...

Table 2—Continued

MSX source name	GLIMPSE source name	Coordinates		2MASS			IRAC					MSX			MIPS	MSX \sum var ^a	IRAS Var
		α (J2000) °	δ (J2000) °	F _J mJy	F _H mJy	F _{K_s} mJy	F _{3.6} mJy	F _{4.5} mJy	F _{5.8} mJy	F _{8.0} mJy	F _{8.28} mJy	F _{12.13} mJy	F _{14.65} mJy	F _{21.3} mJy	F ₂₄ mJy	mJy	
G345.0962−00.7586	SSTGLMC G345.0958−00.7590	256.94200	−41.73290	14.5	84.5	197.7	207.2	159.8	165.3	135.8	310.6	250.9	0	...
G345.3782+00.1131	SSTGLMC G345.3779+00.1130	256.24140	−40.98260	3.1	58.2	239.0	294.0	295.6	350.7	340.6	741.3	862.4	0	...
G345.4913+00.2030	SSTGLMC G345.4911+00.2030	256.23750	−40.83810	...	30.3	184.8	969.8	936.7	495.7	1490.5	1	...
G345.5674+00.2088	SSTGLMC G345.5670+00.2085	256.29220	−40.77400	...	10.5	83.0	888.2	865.4	410.5	921.0	1	...
G345.7172+00.8166	SSTGLMC G345.7172+00.8166	255.77680	−40.28580	47.7	422.5	1134.0	1320.0	556.5	...	1231.0	7388.7	...	0	−1
G345.8705−00.3653	SSTGLMC G345.8703−00.3653	257.13929	−40.87730	28.0	170.7	413.7	431.5	343.8	336.0	278.6	605.0	275.8	0	...
G346.0817−00.7098	SSTGLMC G346.0812−00.7104	257.67180	−40.91250	34.1	164.1	357.4	296.4	218.1	221.3	200.5	511.7	490.8	1	...
G346.1049−00.4608	SSTGLMC G346.1045−00.4611	257.42520	−40.74600	6.2	142.6	400.8	987.6	1562.0	3734.7	4434.5	4016.8	3060.2	1499.3	0	8
G346.1105+00.1244	SSTGLMC G346.1099+00.1241	256.81200	−40.39159	0.7	16.4	97.2	1600.0	1426.0	592.4	1335.1	1497.6	1	...
G346.1675−00.6678	SSTGLMC G346.1671−00.6680	257.69440	−40.81850	3.0	11.2	27.9	125.0	143.5	190.5	230.1	525.4	401.3	1	...
G346.3216−00.0967	SSTGLMC G346.3208−00.0971	257.21050	−40.35500	...	2.8	13.4	1653.0	1361.0	291.1	200.0	1	...
G346.3403−00.1348	SSTGLMC G346.3398−00.1347	257.26519	−40.36270	30.5	194.2	597.5	794.5	888.0	2445.3	2687.1	2236.9	1609.3	1700.7	2	...
G346.4454−00.8279	SSTGLMC G346.4449−00.8282	258.08160	−40.68891	851.8	963.8	483.3	1001.1	482.6	0	0
G346.5687+00.6211	SSTGLMC G346.5685+00.6212	256.65340	−39.72690	10.2	99.4	342.2	343.9	315.0	378.2	365.2	757.0	1274.8	869.9	0	...
G346.6010−00.8760	SSTGLMC G346.6005−00.8763	258.25350	−40.59140	18.7	111.1	270.1	354.4	299.6	293.7	258.4	799.6	358.1	0	...
G346.6367+00.3491	SSTGLMC G346.6367+00.3490	256.98960	−39.83590	48.0	269.6	612.5	1065.0	870.5	483.9	382.0	0	...
G346.7352−00.2706	SSTGLMC G346.7348−00.2705	257.71591	−40.12590	739.4	924.4	495.2	...	807.4	...	864.5	0	...
G346.9036−00.7823	SSTGLMC G346.9029−00.7826	258.38710	−40.29130	11.1	79.1	225.7	227.7	217.2	263.9	320.7	870.6	667.3	0	48
G346.9537+00.7198	SSTGLMC G346.9536+00.7196	256.85111	−39.35990	319.1	353.3	264.0	627.6	535.4	0	...
G347.0772−00.6881	SSTGLMC G347.0764−00.6885	258.42030	−40.09560	19.4	146.9	471.1	769.1	893.0	2333.4	2984.5	2561.1	...	1164.7	2	0
G347.1359+00.7508	SSTGLMC G347.1359+00.7509	256.96010	−39.19550	4.6	63.0	304.5	387.4	...	580.2	654.3	1729.4	1894.3	1771.8	...	771.4	0	−1
G347.2053−00.0780	SSTGLMC G347.2046−00.0781	257.87590	−39.63299	210.5	654.5	1133.0	986.6	782.7	1510.7	1437.6	459.4	1	...
G347.3555−00.2296	SSTGLMC G347.3548−00.2298	258.14989	−39.60100	145.5	369.7	592.0	...	442.9	397.5	330.7	648.0	338.9	0	...
G347.4212+00.3208	SSTGLMC G347.4209+00.3207	257.62530	−39.22280	6.0	98.9	385.4	1360.0	1340.0	627.9	925.4	1	...
G347.4624−00.7491	SSTGLMC G347.4616−00.7491	258.77860	−39.81870	80.8	494.2	1212.0	1048.0	1282.0	4793.1	5564.0	4316.8	4099.3	2831.6	1	...
G347.5235+00.3586	SSTGLMC G347.5229+00.3586	257.66420	−39.11800	1085.0	870.7	391.7	325.2	0	...
G347.5847+00.3636	SSTGLMC G347.5845+00.3635	257.70580	−39.06570	15.7	190.7	648.5	1224.0	1222.0	611.2	...	1067.9	...	795.3	0	...
G347.6554+00.5490	SSTGLMC G347.6549+00.5488	257.56760	−38.89890	9.0	209.0	345.5	488.5	533.5	254.8	383.0	0	...
G347.6742−00.2004	SSTGLMC G347.6737−00.2006	258.36180	−39.32600	32.1	189.4	498.4	1231.0	1283.0	648.0	500.4	1	...
G347.7213+00.1056	SSTGLMC G347.7208+00.1056	258.07780	−39.10790	...	2.7	45.6	226.8	363.7	541.8	590.6	1342.7	1880.8	2233.6	1972.5	990.8	0	...
G348.0423+00.3339	SSTGLMC G348.0422+00.3338	258.08390	−38.71410	1.4	163.4	394.5	787.1	812.2	447.9	1411.6	0	...
G348.0707−00.1019	SSTGLMC G348.0704−00.1021	258.55831	−38.94690	728.9	804.6	1905.5	2384.5	1884.3	1925.6	1655.4	3	...
G348.0866+00.0901	SSTGLMC G348.0863+00.0901	258.37020	−38.82150	16.4	156.0	529.6	829.7	789.3	1986.7	2671.8	2423.8	2640.6	2212.5	0	99
G348.1554+00.1424	SSTGLMC G348.1551+00.1427	258.36770	−38.73520	8.5	70.1	235.9	916.2	1027.0	490.7	901.0	0	...
G348.2111−00.6119	SSTGLMC G348.2110−00.6116	259.19750	−39.12960	225.8	818.7	1623.0	1442.0	1463.0	3493.5	3439.1	2558.1	2101.4	1066.4	0	...
G348.2569−00.0214	SSTGLMC G348.2566−00.0213	258.61421	−38.74880	4.0	43.0	184.3	332.0	...	552.2	605.0	1219.6	...	1408.7	...	1240.6	0	8
G348.3436+00.0360	SSTGLMC G348.3435+00.0361	258.61939	−38.64490	14.9	113.7	325.3	1223.0	1206.0	608.9	474.7	0	...
G348.3901−00.6431	SSTGLMC G348.3899−00.6433	259.36350	−39.00160	38.3	199.7	413.7	422.4	381.9	414.0	407.1	968.4	659.8	0	...
G348.4530+00.9143	SSTGLMC G348.4529+00.9142	257.79550	−38.03999	19.5	99.8	230.5	259.5	216.7	246.1	238.2	671.1	296.1	0	...
G348.4724−00.8122	SSTGLMC G348.4722−00.8122	259.60241	−39.03190	109.0	...	446.1	466.8	459.0	222.6	265.1	1	0
G348.6399−00.3293	SSTGLMC G348.6396−00.3296	259.22050	−38.61640	...	8.6	55.4	219.5	265.5	369.9	470.3	1457.6	1671.9	1381.6	...	1210.6	0	26
G348.6477+00.1834	SSTGLMC G348.6475+00.1832	258.69331	−38.31190	1.2	39.0	242.7	1072.0	952.3	361.5	414.5	1	...
G348.7820+00.5370	SSTGLMC G348.7821+00.5370	258.42840	−37.99620	3.5	34.0	153.2	1000.0	795.2	403.5	141.2	0	...
G348.8250−00.3358	SSTGLMC G348.8246−00.3357	259.36399	−38.46910	71.1	464.2	1146.0	1414.0	1481.0	824.7	801.4	1	...
G348.8440−00.7723	SSTGLMC G348.8437−00.7727	259.83460	−38.70490	50.5	107.1	199.5	269.6	319.1	353.5	421.4	817.9	1067.7	1326.0	2	...
G348.8511−00.5668	SSTGLMC G348.8510−00.5670	259.62460	−38.58100	37.0	121.1	226.5	394.1	271.9	245.9	186.9	398.2	95.4	0	...
G348.8799−00.0639	SSTGLMC G348.8795−00.0639	259.12179	−38.26700	30.4	91.4	111.9	420.0	...	1006.0	923.5	399.9	225.9	1	...
G349.0229−00.5300	SSTGLMC G349.0232−00.5297	259.71230	−38.41930	105.3	454.5	944.3	1029.0	771.6	374.9	256.5	1	...
G349.1085+00.5178	SSTGLMC G349.1084+00.5178	258.69001	−37.74260	34.3	204.5	479.0	458.0	449.9	1147.6	1648.0	882.4	...	944.0	1	...

Table 2—Continued

MSX source name	GLIMPSE source name	Coordinates		2MASS			IRAC					MSX			MIPS	MSX $\sum \text{var}^a$	IRAS Var
		α (J2000) °	δ (J2000) °	F _J mJy	F _H mJy	F _{K_s} mJy	F _{3.6} mJy	F _{4.5} mJy	F _{5.8} mJy	F _{8.0} mJy	F _{8.28} mJy	F _{12.13} mJy	F _{14.65} mJy	F _{21.3} mJy	F ₂₄ mJy		
G349.1628−00.8271	SSTGLMC G349.1623−00.8270	260.12560	−38.47491	21.3	110.4	273.4	422.3	378.4	1028.5	1125.5	336.2	0	0
G349.1967+00.1474	SSTGLMC G349.1962+00.1474	259.13630	−37.88630	...	19.2	100.6	1074.0	1012.0	414.3	544.9	1	...
G349.2236+00.2746	SSTGLMC G349.2236+00.2747	259.02499	−37.79060	353.8	312.3	340.7	262.8	637.8	903.5	486.4	1	...
G349.3072+00.3698	SSTGLMC G349.3072+00.3702	258.98831	−37.66720	113.4	387.9	851.8	1133.0	310.4	661.5	0	...
G349.3584+00.0257	SSTGLMC G349.3583+00.0256	259.38060	−37.82480	32.8	1272.0	1293.0	594.4	...	868.8	...	1046.6	1	...
G349.4256−00.4641	SSTGLMC G349.4252−00.4638	259.93770	−38.05170	84.7	342.2	631.4	367.3	292.5	281.9	225.2	418.0	400.7	1	...
G349.5661−00.1909	SSTGLMC G349.5656−00.1908	259.75620	−37.77990	1252.0	1181.0	553.8	1	...
G349.6145−00.5339	SSTGLMC G349.6142−00.5341	260.14739	−37.93660	2.5	18.5	76.7	1278.0	1448.0	392.2	...	665.3	...	1346.6	0	...
G349.6838−00.6170	SSTGLMC G349.6837−00.6165	260.28410	−37.92710	1.7	26.2	116.1	774.8	895.2	421.2	517.3	0	...
G349.7012−00.9323	SSTGLMC G349.7008−00.9319	260.62590	−38.09200	4.0	225.4	...	895.6	1110.0	521.3	329.0	0	37
G349.7118−00.0586	SSTGLMC G349.7113−00.0585	259.72510	−37.58460	836.0	632.1	336.5	0	...
G349.7760+00.7641	SSTGLMC G349.7762+00.7644	258.92760	−37.05660	49.0	202.3	388.6	367.3	281.3	250.1	191.4	374.0	1	...
G349.8351−00.4089	SSTGLMC G349.8350−00.4088	260.17690	−37.68420	4.5	65.9	259.6	1214.0	1291.0	760.4	782.8	1	...

^aAs defined in Table 3

Note. — The uncertainties are not shown for clarity. However, these are bright sources at mid-IR wavelengths in the *Spitzer* data, and therefore the uncertainties are very low in IRAC and MIPS 24.0 μm . In fact, the main source of uncertainty at IRAC and MIPS 24.0 μm wavelengths are likely to be the calibration uncertainties. For MSX data, one of the requirements used in Section 3.3 was the uncertainty at 8.28 μm should be less than 10%. For the JHK and MSX errors we refer the reader to the original catalogs. The IRAC 8.0 μm flux calculated from the smoothed mosaics is not shown, but for sources to be in this list we required the original IRAC 8.0 μm flux to agree with our calculated IRAC 8.0 μm flux from smoothed mosaics by less than 20%. Finally, we note that this table does not show all fluxes present in the original MSX Catalog (i.e. fluxes have been removed when a source was not seen, or seen with a very low signal-to-noise, in the images).

Table 3. Comparison to previously suspected variables

	All	MSX sources $\sum \text{var} \geq 1^{\text{a}}$	$\sum \text{var} \geq 2^{\text{a}}$	IRAS sources (matched) All	Var > 95%
Initial source list	50744	8783 (17.3%)	504 (1.0%)	2695	207 (7.7%)
Variable candidates	552	236 (42.8%)	35 (6.3%)	95	26 (27.4%)
Highly likely candidates	40	17 (42.5%)	5 (12.5%)	15	7 (46.7%)

^aWe define $\sum \text{var} = \text{vara} + \text{varc} + \text{vard} + \text{vare}$, i.e. the sum of the variability flags for bands A, C, D, and E from the MSX Point-Source Catalog

Table 4. The 40 sources with secondary indicators of variability

MSX source name	GLIMPSE source name
Large $8\mu\text{m}$ variability	
G010.6179–00.0560	SSTGLMC G010.6180–00.0559
G019.6672–00.7858	SSTGLMC G019.6675–00.7870
G301.0439+00.0582	SSTGLMC G301.0440+00.0576
G328.3644+00.3438	SSTGLMC G328.3647+00.3434
G334.9467–00.4008	SSTGLMC G334.9466–00.4005
G337.0848–00.5550	SSTGLMC G337.0848–00.5550
G339.2514–00.3656	SSTGLMC G339.2511–00.3650
G342.7817–00.6938	SSTGLMC G342.7819–00.6937
G346.3216–00.0967	SSTGLMC G346.3208–00.0971
G349.3072+00.3698	SSTGLMC G349.3072+00.3702
G349.6145–00.5339	SSTGLMC G349.6142–00.5341
MSX $21.3\mu\text{m}$ and MIPS $24.0\mu\text{m}$ mismatch	
G012.8758+00.8954	SSTGLMC G012.8754+00.8952
G018.1666+00.7366	SSTGLMC G018.1665+00.7365
G026.8076–00.3922	SSTGLMC G026.8077–00.3920
G031.6975–00.3260	SSTGLMC G031.6973–00.3259
G033.4658+00.8407	SSTGLMC G033.4657+00.8406
G036.2908–00.0402	SSTGLMC G036.2906–00.0404
G064.9674+00.4695	SSTGLMC G064.9676+00.4696
G296.6843+00.4515	SSTGLMC G296.6844+00.4513
G319.8400+00.0308	SSTGLMC G319.8394+00.0312
G336.8569+00.6024	SSTGLMC G336.8563+00.6026
G338.2051–00.3526	SSTGLMC G338.2049–00.3525
G338.7552+00.6664	SSTGLMC G338.7552+00.6663
G343.7460–00.5851	SSTGLMC G343.7460–00.5851
G346.1049–00.4608	SSTGLMC G346.1045–00.4611
Mismatch between JHK_s and IRAC	
G010.9867+00.1010	SSTGLMC G010.9866+00.1011
G017.5692–00.0692	SSTGLMC G017.5696–00.0693
G017.6991–00.1976	SSTGLMC G017.6993–00.1978

Table 4—Continued

MSX source name	GLIMPSE source name
G017.9268+00.4932	SSTGLMC G017.9269+00.4933
G020.3407+00.4617	SSTGLMC G020.3405+00.4618
G020.4301–00.1046	SSTGLMC G020.4305–00.1044
G034.8787–00.5619	SSTGLMC G034.8785–00.5622
G035.8416+00.5887	SSTGLMC G035.8411+00.5890
G318.9134+00.7526	SSTGLMC G318.9131+00.7530
G322.4192–00.0746	SSTGLMC G322.4196–00.0744
G325.5458–00.3432	SSTGLMC G325.5463–00.3436
G329.9308–00.2980	SSTGLMC G329.9310–00.2982
G330.5727–00.6220	SSTGLMC G330.5728–00.6218
G334.8128–00.1059	SSTGLMC G334.8125–00.1053
G335.4507+00.0785	SSTGLMC G335.4500+00.0789